DETERMINATION OF pP AND sP DELAYS FROM SEISMIC CODAS

Edward A. Page

ENSCO, Incorporated

Prepared for:

Air Force Technical Applications Center
Advanced Research Projects Agency

31 March 1974

16 April 1973 F234.7

DEPARTMENT OF DEFENSE FORMS

F-200.1473 *DD Form 1473:* Report Documentation Page

AD-784348

SECURITY CLASSIFICATION OF THIS PAGE (When Data Entered)

REPORT DOCUMENTATION PAGE	READ INSTRUCTIONS BEFORE COMPLETING FORM
1. REPORT NUMBER / 2. GOVT ACCESSION NO	3. RECIPIENT'S CATALOG NUMBER
4. TITLE (and Subtitle): Determination of pP and sP delays from seismic codas	5. TYPE OF REPORT & PERIOD COVERED: Final Report 6. PERFORMING ORG. REPORT NUMBER: N/A
7. AUTHOR(s): Edward Page	8. CONTRACT OR GRANT NUMBER(s): F08606-74-C-0020
9. PERFORMING ORGANIZATION NAME AND ADDRESS: ENSCO, INC. 8001 Forbes Pl., Spfld., Va.	10. PROGRAM ELEMENT, PROJECT, TASK AREA & WORK UNIT NUMBERS
11. CONTROLLING OFFICE NAME AND ADDRESS: DCASD, Baltimore Bldg. 22, Fort Holabird Baltimore, Maryland 21219	12. REPORT DATE: 31 March 1974 13. NUMBER OF PAGES: 57
14. MONITORING AGENCY NAME & ADDRESS (if different from Controlling Office): VELA Seismological Center 312 Montgomery Street Alexandria, Virginia 22314	15. SECURITY CLASS. (of this report) 15a. DECLASSIFICATION/DOWNGRADING SCHEDULE
16. DISTRIBUTION STATEMENT (of this Report): APPROVED FOR PUBLIC RELEASE. DISTRIBUTION UNLIMITED.	
17. DISTRIBUTION STATEMENT (of the abstract entered in Block 20, if different from Report)	
18. SUPPLEMENTARY NOTES	
19. KEY WORDS (Continue on reverse side if necessary and identify by block number): Seismic depth, depth phase, echo detection	
20. ABSTRACT (Continue on reverse side if necessary and identify by block number): Work was performed to determine the feasibility of making significant improvements in seismic depth phase detection using statistical signal processing. The feasibility was demonstrated for a single event analyzed at six stations.	

DD FORM 1473 EDITION OF 1 NOV 65 IS OBSOLETE

SECURITY CLASSIFICATION OF THIS PAGE (When Data Entered)

F-200.1473

ARMED SERVICES PROCUREMENT REGULATION

Notice of Disclaimer

The views and conclusions contained in this document are those of the author and should not be interpreted as necessarily representing the official policies, either expressed or implied, of the Advanced Research Projects Agency, the Air Force Technical Applications Center, or the U.S. government.

SUBJECT: Determination of pP and sP Delays From Seismic Codas

AFTAC Project No.....VELA T/4710
ARPA Order No.....1620
ARPA Program Code.....4F10
Name of Contractor.....ENSCO, INC.
Contract Number.....F08606-74-C-0020
Effective Date of Contract.....5 September 1973
Report Period.....6 August 1973 to 28 February 1974
Amount of Contract.....$39,441
Contract Expiration Date.....28 February 1974
Project Scientist.....Edward A. Page (703-569-9000)

TABLE OF CONTENTS

1.0 INTRODUCTION

The objective of this research effort was to determine the feasibility of making significant improvements in seismic depth phase detection using statistical signal processing techniques developed at ENSCO, INC. Applications of these techniques together with additional techniques developed in the course of the investigation indicate significant depth phase detection improvements are possible.

The primary interest in detecting seismic depth phases is that good estimates of event depths can be obtained from the (pP-P) and (sP-P) arrival time differences. This type of depth determination is preferred over all other depth estimation procedures.

At present, depth phase detection is usually performed by visual identification from the seismogram and is not successful for many events. This type of detection uses only a very limited portion of the depth phase information contained in the seismogram and is successful only when depth phases are particularly strong. Even when depth phases are visually detected there can be substantial errors in the delay time estimates since they are based on the identification of P, pP, and sP first movements. A procedure which utilizes a larger portion of the P, pP and sP waveforms would provide a more precise estimate.

To date, depth phase detection based on techniques such as the auto-correlation, cepstrum, etc. have also had limited success. Although these techniques use more of the information contained in the seismogram, detection commonly deteriorates rather than improves when more of the coda is used in the analysis.

The statistical processing techniques which we have developed are based on simple physical models and insure constructive use of the depth phase information contained in the entire seismogram. These new techniques are:

1. Stochastic stacking - this technique allows for depth phase delay time variations along the coda which are associated with the later seismic arrivals.

2. Phase stacking - the consistency of the phase difference between the direct and reflected waves can be used to enhance depth phase detection.

Recordings of a seismic event were analyzed at six stations using the new statistical techniques as well as several of the conventional techniques. For the event analyzed, the depth phases were not visually apparent. The conventional signal processing techniques detected the pP at one of the six stations whereas the new techniques detected both the pP and sP at one station, and the pP at two others.

It was also determined that by stochastically averaging the data from several stations depth phases could be detected that were not apparent from analysis of the data from any of the individual stations.

The results based on this work indicate that these new techniques could greatly increase the frequency and accuracy of the detection of seismic depth phase delay times.

2.0 SEISMIC DEPTH PHASE DETECTION

2.1 Simplified Geophysical Model

The simplified geophysical model illustrated in Figure 1, can help indicate some of the problems associated with using the entire record for seismic depth phase detection.

In general, a seismogram is constructed of seismic arrivals taking many different paths from source to receiver. The first of these seismic arrivals is the direct P wave followed by its associated reflected phases pP and sP, which arrive along minimum time paths very similar to that of the P wave for event depths of ~50 km or less. It is the arrival time differences of these first three arrivals which are most useful for depth determination. (In Figure 2 are examples of seismic recordings for which the P, pP and sP phases are easily identified.) At some later point in time seismic waves which reflect off the core arrive as PcP, pPcP and sPcP phases. Later yet (depending on the event location) PP, pPP and sPP phases will arrive. The point here is that the seismogram is constructed of triplets of arrivals from each of the many seismic paths from source to receiver. In general the time delays within these triplets will differ since the relative geometry of the paths within each triplet is different. The consequence of this is that the depth phase delay time will vary as a function of position along the coda. As an example, for a 40 km event at 45°, the pP-P delay

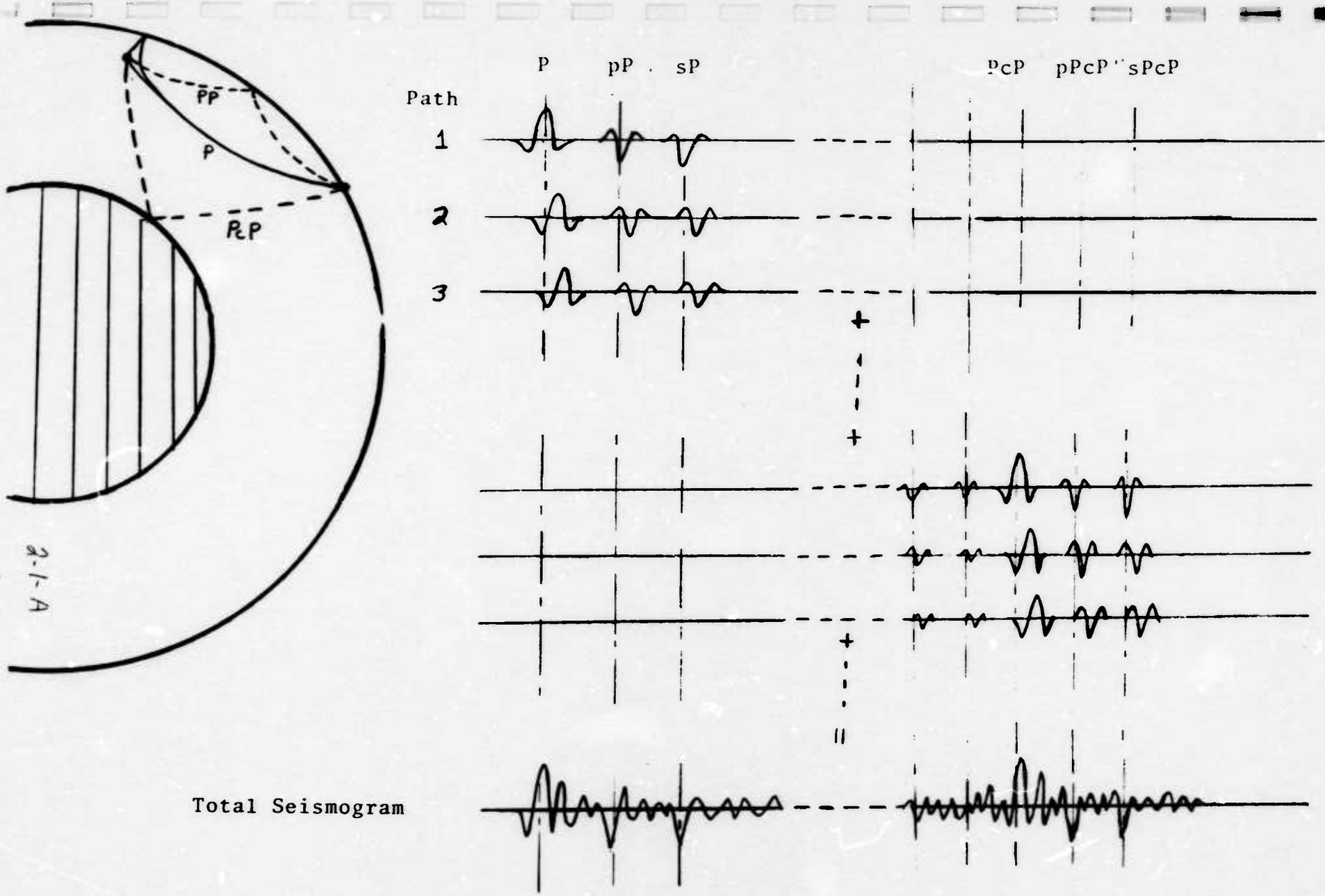

Simplified Geophysical Model

Figure 1

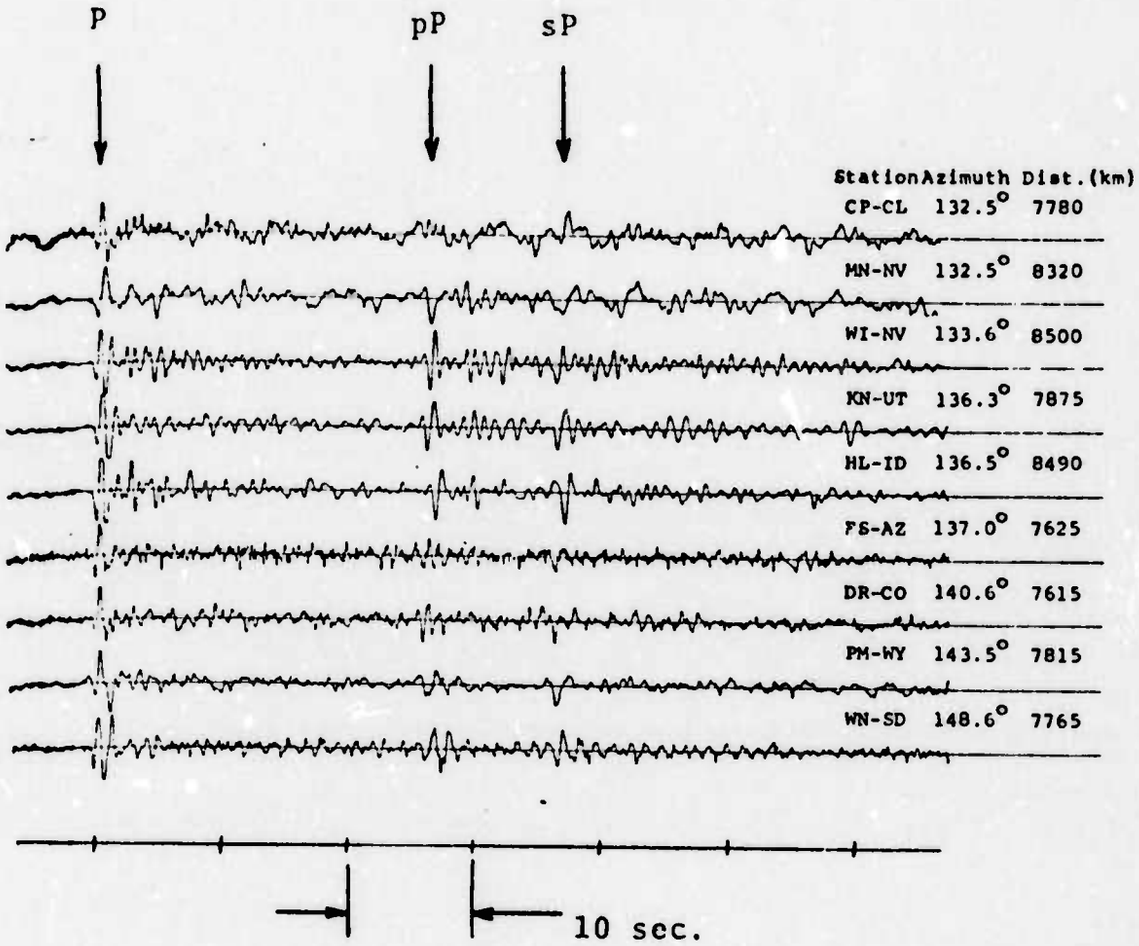

Figure 2: Example Unfiltered Z-Component Seismograms showing Initial Phases (Bolivia Event 12:02:22 Z 19 July 1962)

is ~11 sec. whereas the pPP-PP delay is ~10 sec. Adjusting for these variations by use of travel time tables is not an obvious procedure since the relative strength of the various overlapping phases and the event depth must be approximately known.

To see how such delay time variations can deteriorate depth phase detection, consider the cepstrum analysis of a synthetic seismogram. The cepstrum is a near optimum echo detector for Gaussian echoed signals in Gaussian noise.[1,2] In Figure 3 are the cepstrums of synthetic seismograms for events at 40 and 15 km depth; the horizontal axis is time in seconds. The synthetic seismograms were generated by passing white noise through a recursive digital filter having a band pass typical for seismic arrivals and adding this signal to itself at delays τ_1 and τ_2(corresponding to pP-P and sP-P). The recursive digital filter was designed from the following z-transform of a resonator with poles at $z=re^{\pm j\omega_r T}$ and a zero at q;

$$H(z) = \frac{1-qz^{-1}}{(1-2r(\cos\omega_r T)z^{-1} + r^2 z^{-2})}$$

For q=1 this gives zero gain at $\omega=0$ and a resonant response with ω_r determining the resonant frequency and r relating to the Q of the response. We used q=1, r=.9 and $\omega_r=2\pi$ for the generation of the synthetic data with T being the inverse of the sample rate.

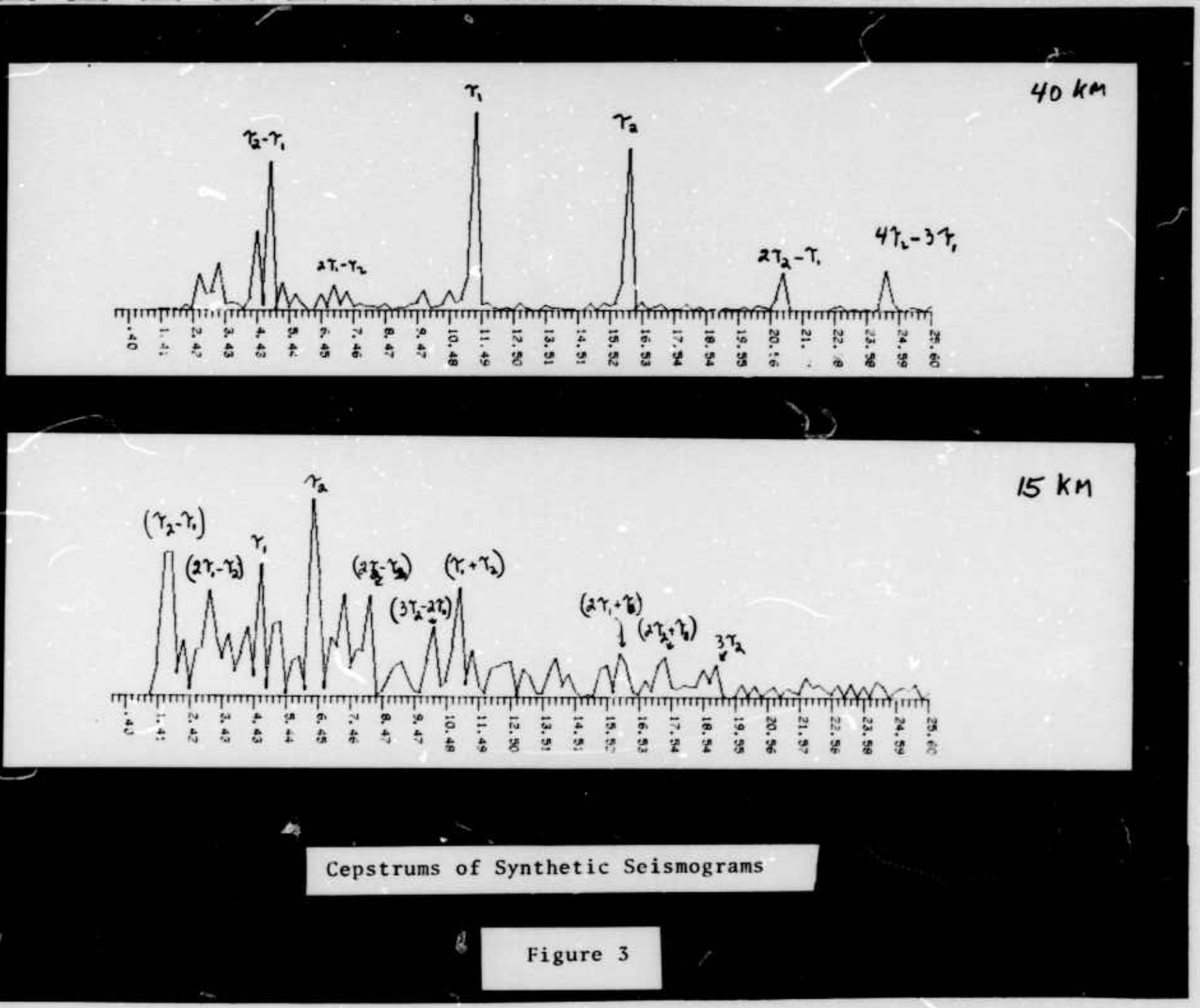

Cepstrums of Synthetic Seismograms

Figure 3

2-3-A

In this simulation the delay times τ_1 and τ_2 were constant throughout the seismogram and clear cepstral peaks indicate the delays τ_1 and τ_2 for the 40 km case. Peaks will also appear at many of the possible combinations of arrival times $(n\tau_1 \pm m\tau_2)$ where n and m are integers. In the 15 km example it is apparent that interpretation of these results should be done using the entire cepstrum pattern.

If τ_1 and τ_2 vary along the seismogram by times comparable to the half widths of the cepstral peaks or greater, the prominence of these peaks would be substantially reduced since their amplitudes would be distributed over a range of delay time values. To compensate for this type of reduction in cepstral peak detection a stochastic stacking technique is used.

2.2 Stochastic Stacking

A stochastic stacking technique can be used to increase the detectability of a peak whose position can vary unpredictably within a certain limited range. To see this, first consider a set of cepstrums calculated from consecutive time segments of a seismogram. If the depth phase delay time were the same in each segment, then by stacking (adding) these cepstrums, the amplitudes of the stationary peaks would add whereas the non-stationary peaks arising from origins other than the depth phase delay times would average to some lesser amplitude level. This is also true for the same calculation of a single cepstrum of the entire seismogram.

By redefining the N cepstrum values x_i, i = 1,N to be

$$y_i = \text{MAX}\ (x_j,\ j = i - \Delta/2,\ i = i + \Delta/2)$$

for each point i, and then by adding the y arrays one can increase detectability for cases in which the peak of interest moves unpredictably within a window Δ. Figure 4 illustrates this technique using synthetic data. Each of the top six arrays are constructed of random numbers having values between 0 and 1. A peak (indicated by an arrow in Figure 4), defined by three points having values .8, 1.2 and .8, is added to each array, but shifted on additional point to the right in each array. The result of adding these arrays (straight stacking) is shown and it is seen that a clear detection of the peak is not achieved by ordinary stacking. However, if before adding, one redefines

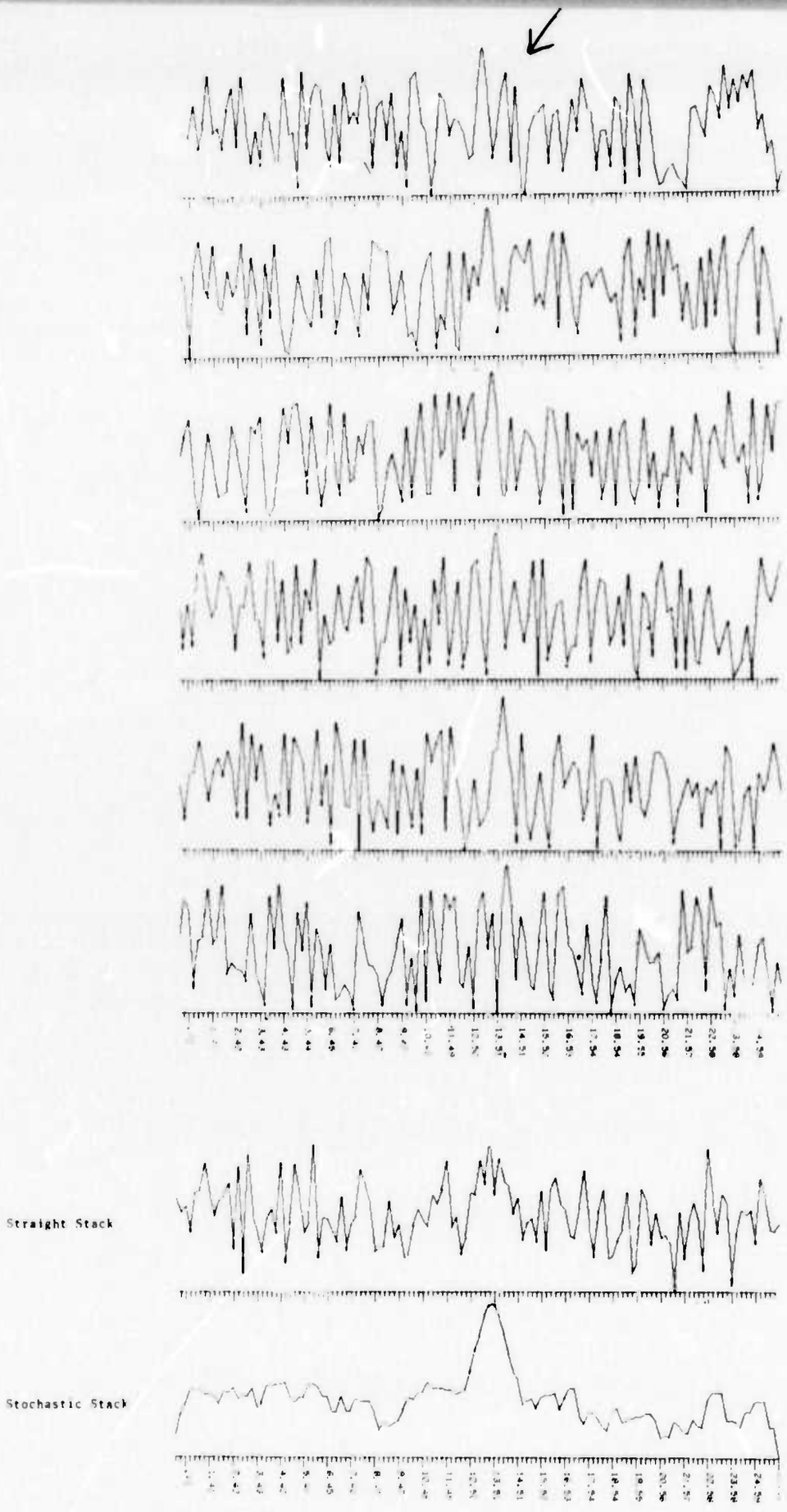

Demonstration of stochastic stacking using synthetic data

2-4-A

Figure 4

these arrays as has been outlined, the results show that a dramatic improvement in peak detection is achieved by using this stochastic stacking procedure. (In Figure A1 of the appendix, one can compare this stochastic stacking procedure with that of low pass filtering the arrays with a cutoff frequency equal to the inverse of the stochastic time window Δ. It is seen that stochastic stacking and linear filtering have different effects on data.)

Thus, the stochastic stacking technique should be effective in detecting depth phase delay times since these delay times vary as a function of position along the seismogram.

2.3 Phasor Stacking

Impressive improvements in seismic depth phase detection, in addition to those gained by stochastic stacking, have been obtained by using information concerning the phase difference between the direct and reflected waves. To see how this can be achieved consider the steps involved in calculating the cepstrum.

Consider the received signal $F(t)$ to be the sum of the direct wave $f(t)$ and a single echo of relative amplitude α, "phase" θ, and echo delay time τ. $F(t)$ can be written

$$F(t) = f(t) + \alpha [f(t - \tau) \cos \theta + f_H (t - \tau) \sin \theta]$$

Here f_H represents the Hilbert transformation of f which corresponds to shifting each Fourier component of f by $\pi/2$. The bracketed expression then represents the signal f(t) having each of its Fourier components shifted by θ. This phase shift θ is the phase difference between the direct and reflected signal. For example, if the echo differed from the direct signal by only a change in sign, θ would equal π.

The power spectrum of F(t) is,

$$P(\omega) = p(\omega)\ [1 + \alpha^2 + 2\alpha \cos\ (\omega\tau - \theta)]$$

for $\omega \geq 0$ and with $p(\omega)$ being the power spectrum of f(t). As can be seen from the expression for $P(\omega)$, the power spectrum $p(\omega)$ is modulated by a cosinusoidal function having frequency τ and phase θ. Taking the complex spectrum of $P(\omega)$ one would then obtain a peak at lag τ which would have phase θ. Therefore one can assign a phase θ to each point of the cepstrum which is calculated by taking the power spectrum of log $P(\omega)$.[2]

To see how this phase information can aid in depth phase detection consider events at ~50 km or less. For such events the direct and reflected phases (e.g., PcP, pPcP, sPcP) travel similar paths once outside the vicinity of the event. It is then reasonable to assume that the direct and reflected phases would undergo similar reflections, distortions, etc. once away from the source region and whatever phase relationship they had emerging from the source region would tend to be preserved in

route to the receiver. If the different reflected phases had undergone similar phase shifts relative to the direct waves, the phase of the depth phase cepstral peaks, calculated from different portions of the seismogram, should tend to be constant within a possible π shift.[3] Spurious cepstral peaks not related to the echo delay times would have a more random phase as a function of which portion of the seismogram is analyzed.

These assumptions are really just generalizations of ideas normally assumed about the direct and reflected waves. It is common to consider the echo to have a waveform similar to the direct wave but having the same or different sign depending on the angle of reflection and on the signs of the parts of the radiation pattern that radiate the direct and the reflected waves. This is equivalent to saying there is a 0 or π phase difference between the direct and reflected waves. What we have done here is to generalize this idea to include all phase shifts from 0 to 2π rather than just 0 and π and to use the consistency of $\theta \pm \pi$ throughout the seismogram to aid the depth phase detection.

This phase consistency can be utilized by stacking cepstrum phasor arrays and computing the amplitudes of the phasor sums. By stacking those phasor arrays cepstral peaks which have a consistent phase $0 \pm \pi$ throughout the stack can become dominant even though their amplitude sums are not. This effect will be demonstrated in the analysis of the data. We also note that the degree of phase selectivity can be adjusted by the manner in which the phasors are summed.

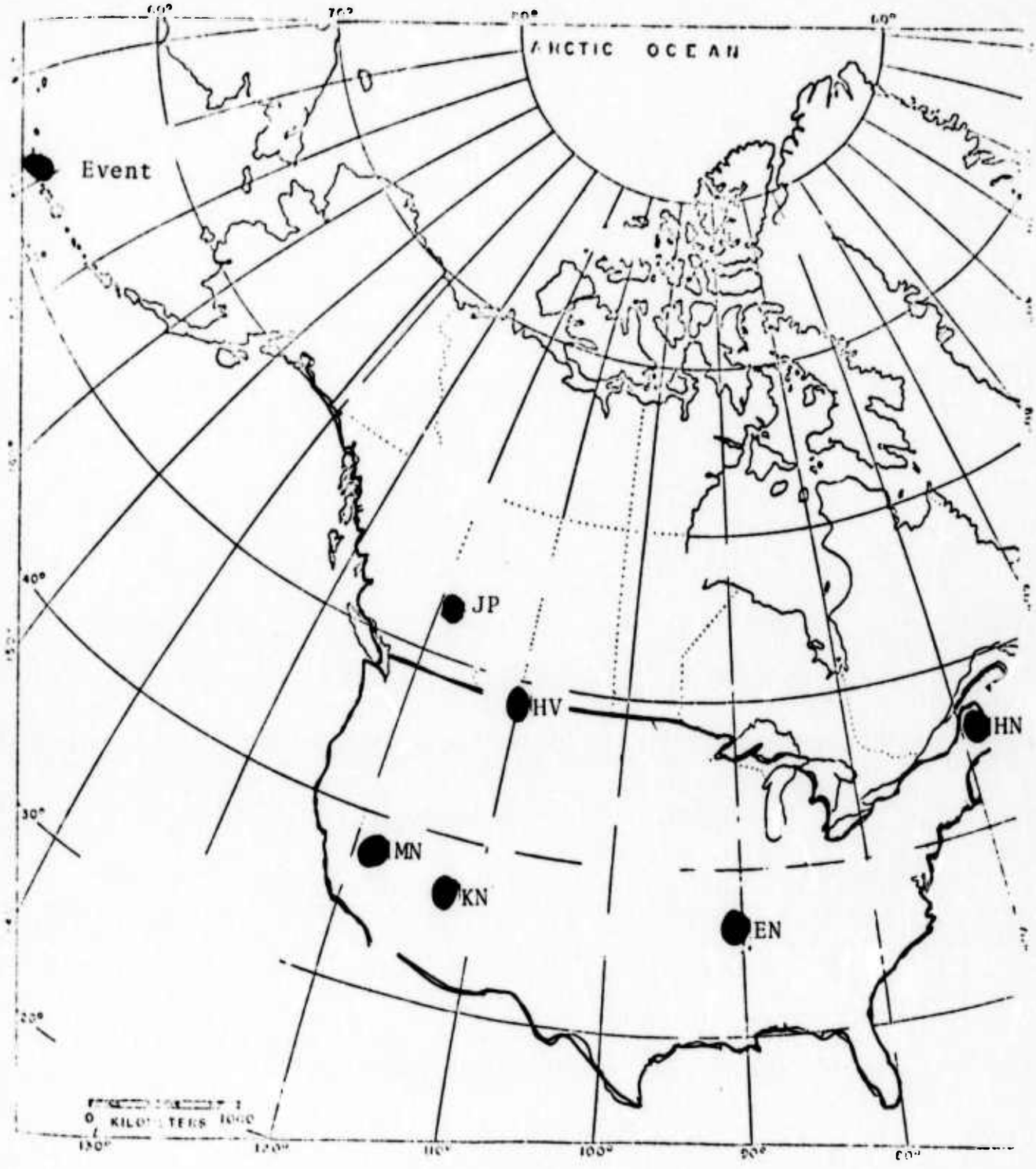

Event and Station Locations

Figure 5

3.0 APPLICATION OF TECHNIQUES TO A SEISMIC EVENT

Analysis was performed on seismic data recorded at six stations for a single event using these new depth phase detection techniques as well as several of the conventional analysis techniques. The event chosen was the Andreanof Island Earthquake of 22/11/65 (origin 2025 31.1, 51.4 N, 179.7 W, m_b = 5.9, sample rate = 20 sps). The map of Figure 5 indicates the event location and the six LRSM stations from which the seismic recordings were analyzed.

C&GS reported this event to have a depth of 40 km from location fit estimates and the results of our analysis agree with this depth estimate. However, the analysis by SDL ("The Long Shot Experiment"),SDL Report 234, Vol. II, page 51) concludes that, "... The visual analysis of the LRSM records across North America for the 22 November 1965 event revealed a depth phase pP which was consistent from station to station and which resulted in a depth calculation of approximately 20 km. ...". If one inspects the records used for this analysis (Fig. 5a) one sees that this is not at all an obvious conclusion. In Figure 5a the dotted lines indicate the approximate positions for pP for an event at 20 km and pP and sP for an event at 40 km. From these records it would be difficult to make conclusions concerning

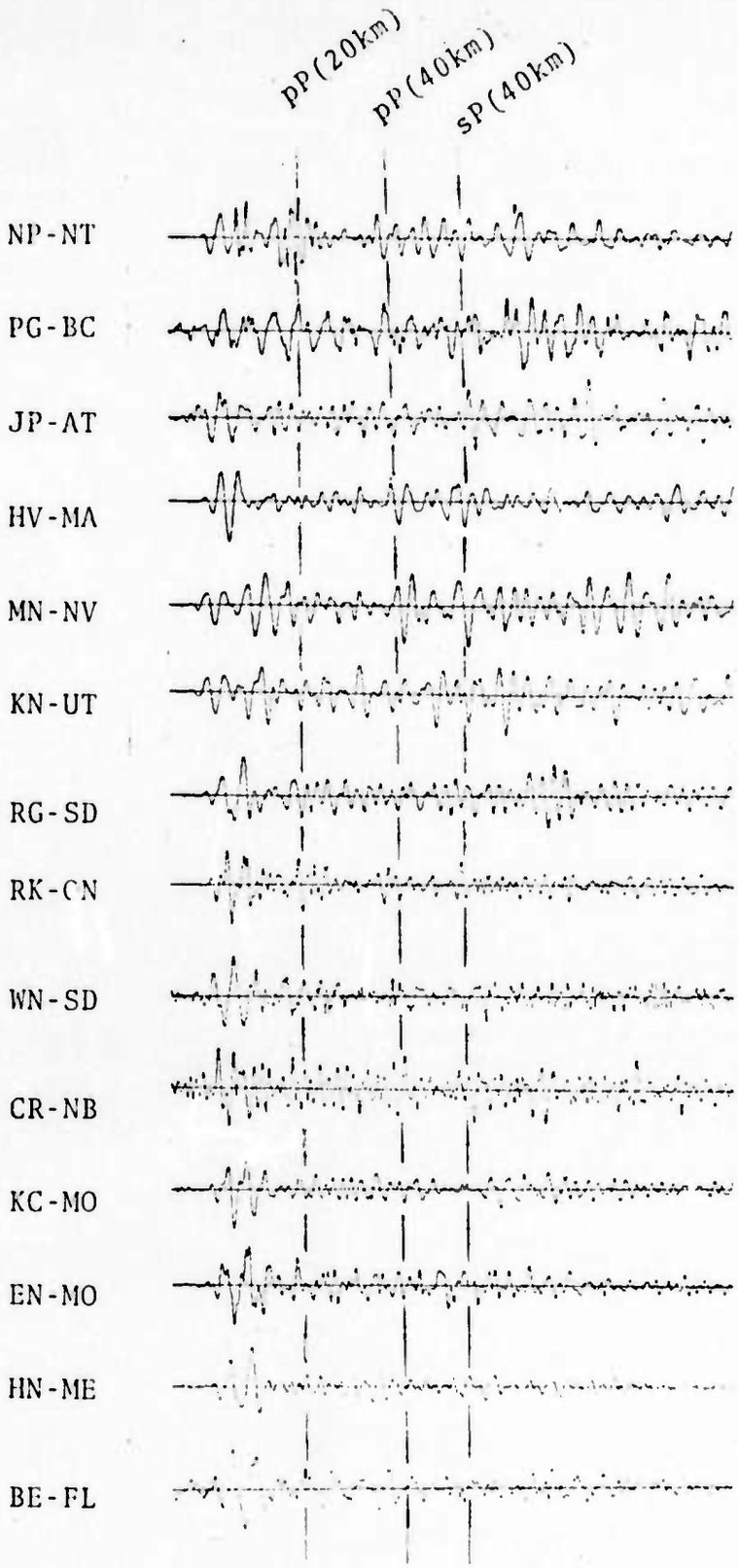

Time Series for 22 Nov.1965 earthquake.

Figure 5a

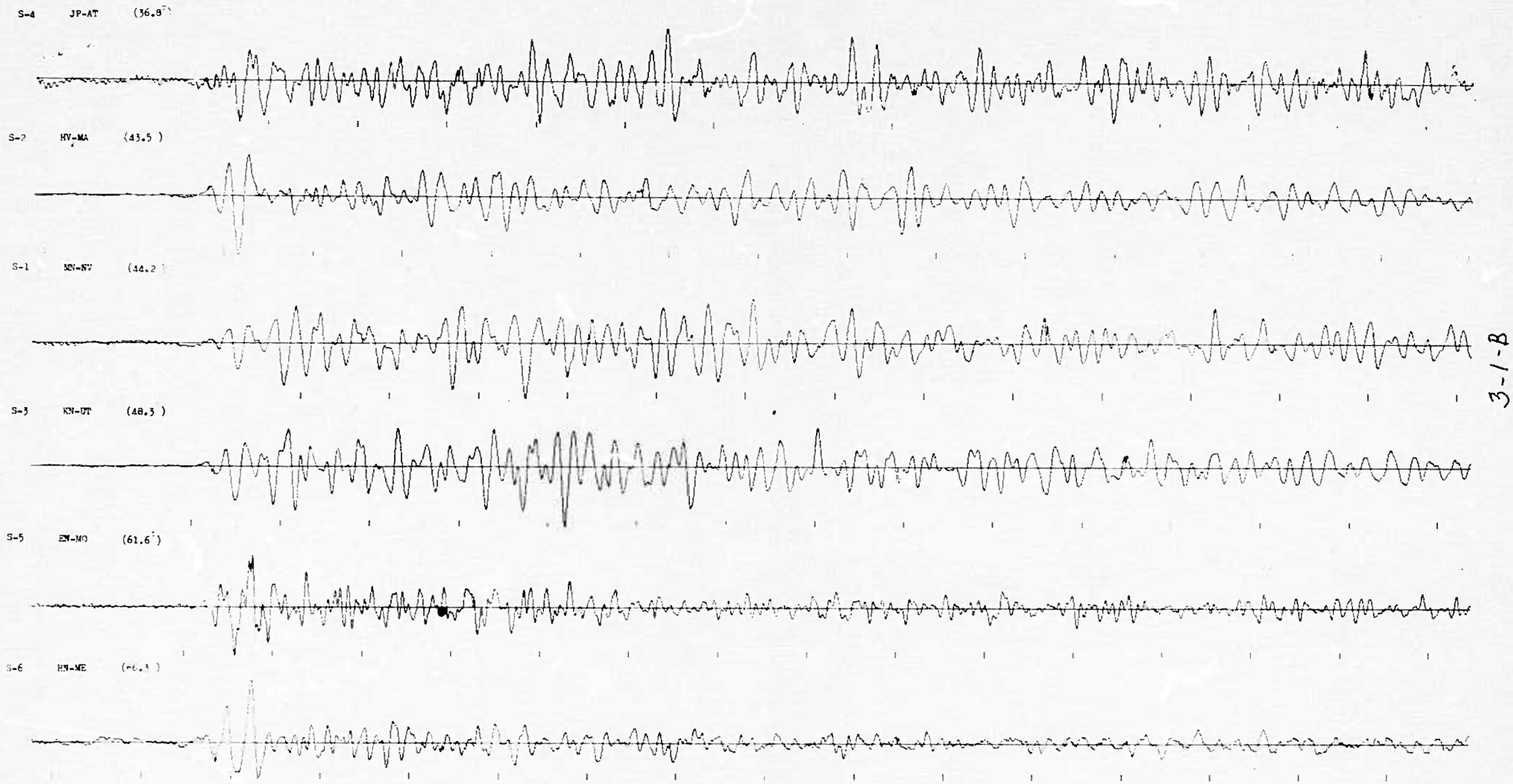

Seismograms (tic mark interval - 5 seconds)

Figure 6

any of the depths. However, if one considers the Bolivian Event (Figure 2) to be a good example of the wave forms received when the depth phases are clearly identifiable, then the records of HV-MA and MN-NV (Figure 5a) would be the most suggestive indication of depth phases and these would be in agreement with the 40 km depth estimate.

The seismograms we analyzed are plotted in Figure 6 and show a good signal to noise ratio eventhough the depth phases are not visually apparent.

Analysis was done using the following methods:

1. Cepstrum of the direct arrival portion of the seismogram (1st - 25.6 sec.)

2. Cepstrum of a ~4 min. portion of the seismogram

3. Stacked cepstrums (9 - 25.6 second samples)

4. Stochastic stacked cepstrums (9 - 25.6 sec. samples)

5. Stochastic cepstrum phasor stack (9 - 25.6 second samples)

Additional methods used for the comparison of low pass filtering to stochastic windowing were:

6. Stacked auto-correlation functions of low pass filtered data (9 - 25.6 second samples)

7. Stacked cepstrum of low pass filtered data (9 - 25.6 second samples)

The following steps used in the calculation of the cepstrum were optimized using the synthetic data:

- Select N sampled (sample rate = 20 pts/sec) amplitude values from the M^{th} portion of a seismogram

  $$X_M(n),\ n=0,\ 1,\ \ldots,\ N-1$$

  and add N zeroes to interpolate the spectrum

- Calculate the amplitude spectrum for positive frequencies

$$A_M(j) = \left| \frac{1}{2N} \sum_{n=0}^{2N-1} X_M(n) e^{-2\pi i n j/2N} \right| ;\ j=0,1,\ldots,\ N-1$$

  with the Nyquist frequency = 10 Hz and $i = (-1)^{1/2}$.

- Retain only the lower quarter of frequencies of the amplitude spectrum since there is very little energy at frequencies above 2.5 Hz. This leaves the array

$$(A_M(j),\ j = 0, 1, \ldots, N/4-1)$$

- Remove the mean and apply a cosinusoidal taper to the first 10% and last 20% of the A_M array giving the modified array

$$(A_M'(j),\ j = 0, 1, \ldots, N/4-1)$$

The 20% taper on the higher frequencies was used to increase the de-emphasis of the higher frequencies and was based on indications from other works [4] that the depth phase spectrum has a greater similarity to the direct phase spectrum below ~1.5 Hz.

- Add N/4 zeroes to interpolate the cepstrum giving the array

$$(A_M'(j),\ j = 0, 1, \ldots, N/2-1)$$

At this stage one would take the log of this A_M' array to obtain the log cepstrum; but our results show that by not using the log better results were obtained and the results presented in this report were all obtained without use of the log.

- Calculate the Fourier Transform of the A_M' array.

$$F_M(k) = \frac{1}{N/2} \sum_{j=0}^{N/2-1} A'_M(j) e^{-2\pi ijk/(N/2)}$$

where $(F_M(k), k = 0, 1, \ldots, N/4-1)$ are

complex numbers representing the positive frequency spectrum of A'_M. One can now obtain the amplitude and phase of each cepstrum point k. The array

$(|F_M(k)|, k = 0, 1, \ldots, N/4-1)$ is what we

refer to as the cepstrum amplitude and the complex numbers $F_M(k)$ are referred to as cepstrum phasors.

- To calculate the stochastic cepstrum stack, one then calculates

$$|F_M(k)| = \text{Max} (|F_M(j)|, j = k-\Delta/2, k+\Delta/2)$$

for each section M and then sums over the number of sections (NS) used from a given seismogram (Δ is the stochastic window width) giving

$$C(k) = \sum_{M=1}^{NS} |F_M(k)| \cdot W_M$$

where C(k) is the stochastic cepstrum stack and W_M is a weighting factor, chosen such that the mean amplitude of each $|F_M(k)|$ array is equal.

- To calculate the stochastic cepstrum phasor stack, each $F_M(k)$ is replaced by $F_M(n)$ where n is the index of the Max value of $|F_M(j)|$ in the interval $j=k-\Delta/2$, $k+\Delta/2$. Then the stochastic cepstrum phasor stack is defined by

$$CP(k) = \left| \sum_{M=1}^{NS} W_M \cdot F_M(k) \right|$$

3.1 Comparison of the New Depth Phase Detection Techniques with the Conventional Methods

We will now compare the effectiveness of the various techniques in detecting depth phases from recordings for which they are not visually apparent. The data from all six stations was processed in the identical fashion. In Figure 7 are the analysis results for the station MN-NV. At the top of the figure is a plot of the first portion of the seismogram. The next three plots are the cepstrums calculated in the three conventional ways indicated. The two vertical dotted lines mark the expected delay times for the pP and sP phases for a 39 km deep event, the depth we determined this event to be. For an event at ~60° these delay times would be ~11.1 and ~15.8 respectively.

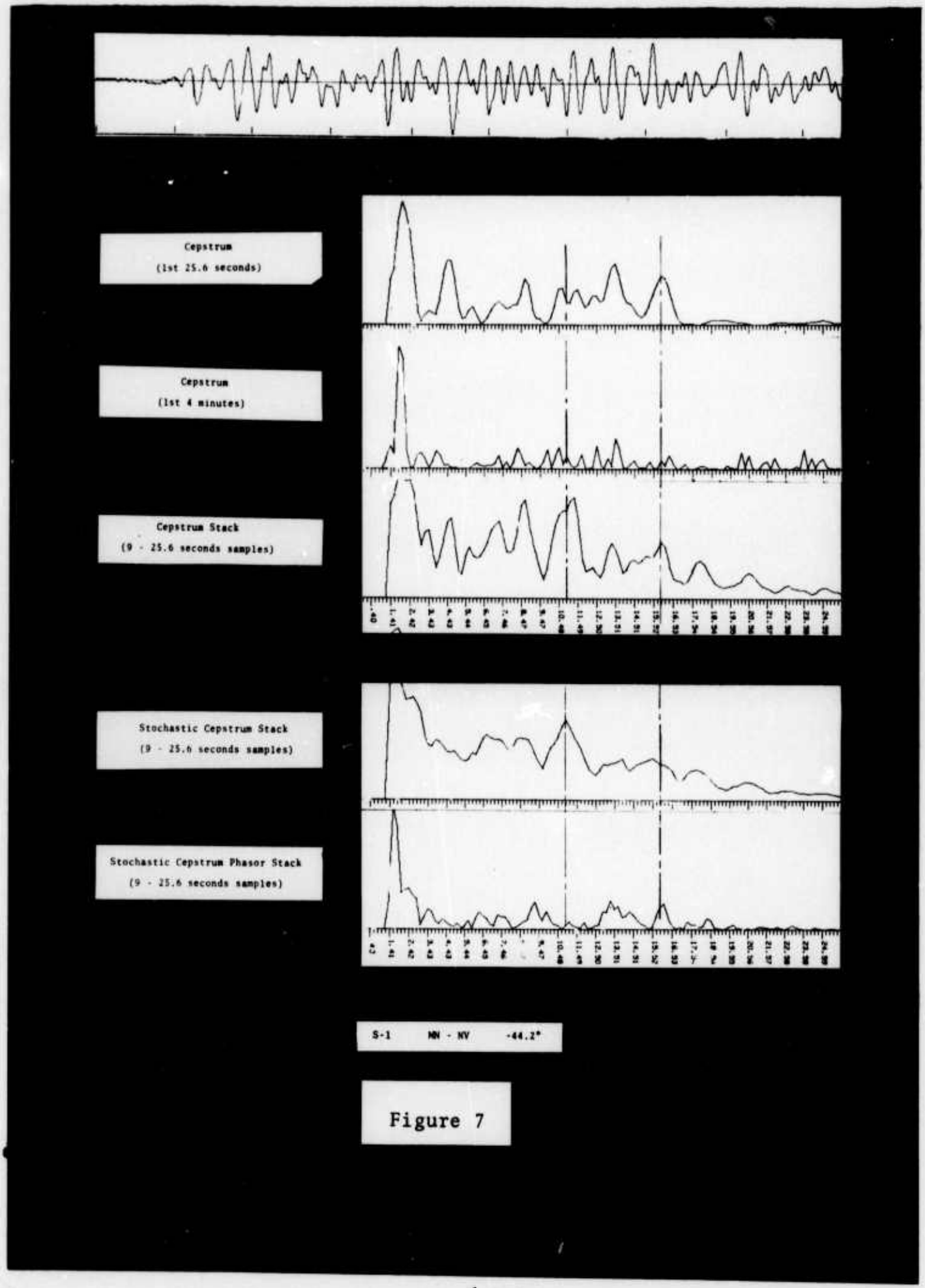
Cepstrum
(1st 25.6 seconds)
Cepstrum
(1st 4 minutes)
Cepstrum Stack
(9 - 25.6 seconds samples)
Stochastic Cepstrum Stack
(9 - 25.6 seconds samples)
Stochastic Cepstrum Phasor Stack
(9 - 25.6 seconds samples)
S-1 MN - NV -44.2°

Figure 7

In interpreting these cepstrums one seeks dominant peaks at the appropriate delay times. In the cepstrum of the 1st - 25.6 seconds of data, a peak appears at the sP time delay; however, it does not stand out from several of the other peaks. Similarly, dominant peaks are not results obtained for the cepstrum of ~4 min. of data and for the cepstrum stack consisting of 9 - 25.6 second samples.

In the next plot down, we see the positive effects of the stochastic stacking technique. The stochastic cepstrum stack uses the identical cepstrums that were used in the cepstrum stack plotted above, but by using this technique the peak at the pP delay time is the dominant peak.

In achieving this the stochastic window was varied from 0. to 1.6 seconds where the results plotted are for a window width of .8 seconds. The results of the stochastic stacking as a function of the various time windows are plotted in Figure 8. We see that the best results are obtained using the windows in the range of .8 and 1.2 seconds. This window width range gave the best results for all stations, and is in agreement with the maximum delay time variation expected. That being the (pP-P) - (pPP-PP) difference of ~1 sec. Thus, it may be possible to estimate what window to use for a given event. (Figure A2 of the appendix shows another example of the effect different stochastic window widths have for the station EN-MO.)

In the stochastic cepstrum phasor stack, shown in the bottom plot, each point of the cepstrum was represented by a phasor and the amplitude of the stochastic cepstrum phasor sum was plotted. This technique was not effective for this station for reasons to be discussed.

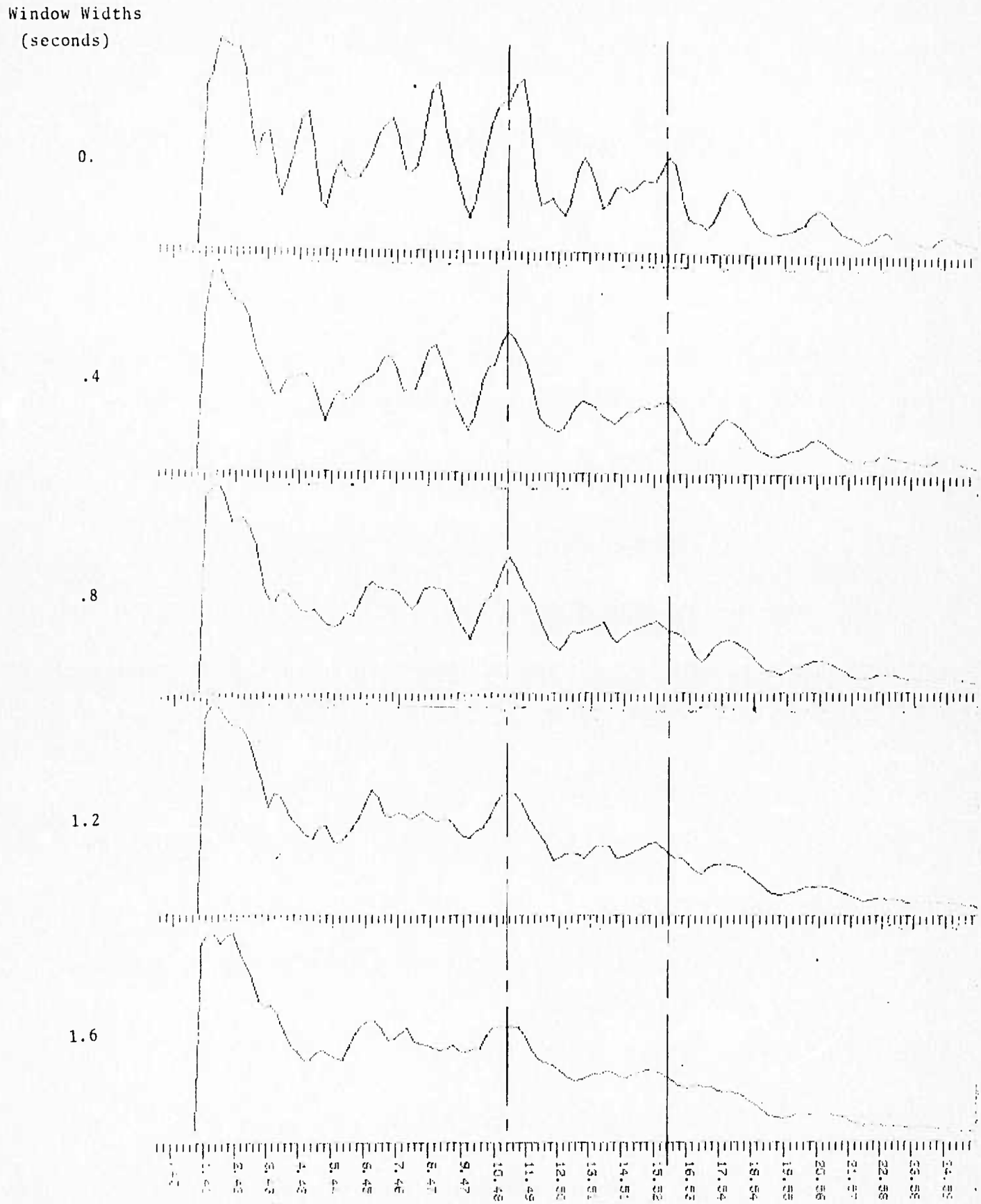

Stochastic cepstrum stack for various
stochastic window widths (MN-NV)

3-7-A

Figure 8

Next consider the results for HN-ME shown in Figure 9. Here again the first three conventional cepstrums analysis techniques did not produce dominant peaks at either of the expected pP and sP delay times. In this case the addition of stochastic stacking was not enough to improve on the normal techniques. However, here the combination of the phasor technique with the stochastic stacking resulted in the detection of peaks at both pP and sP delay times. (The phasor stacking gave these results only when used with the stochastic windowing.) In fact the entire cepstrum pattern of the stochastic cepstrum phasor stack is in agreement with the cepstrum (bottom plot) calculated from a synthetic seismogram for this event. The single station analysis, giving the entire cepstrum pattern expected for an event at ~39 km, is by itself extremely strong evidence for an event at this depth. We will see that these results are in agreement with the other depth determinations to be discussed.

The reason the phasor techniques failed using data from MN-NV is now understood. As was discussed in Section 2.3, there is the possibility of the phase difference θ to change by π along the coda.[3] This was, in fact, observed in examination of the phase as a function of position along the coda. The phasor stack was then changed to constructively add phasors π out of phase and a detection comparable to the stochastic stack of MN-NV was achieved.

The amplitude of the individual cepstrum phasor arrays for HN-ME is plotted in Figure 10. Consider the peak at the sP delay time in the bottom plot of the phasor array sums. By inspecting the amplitudes at this delay time for each of the 9

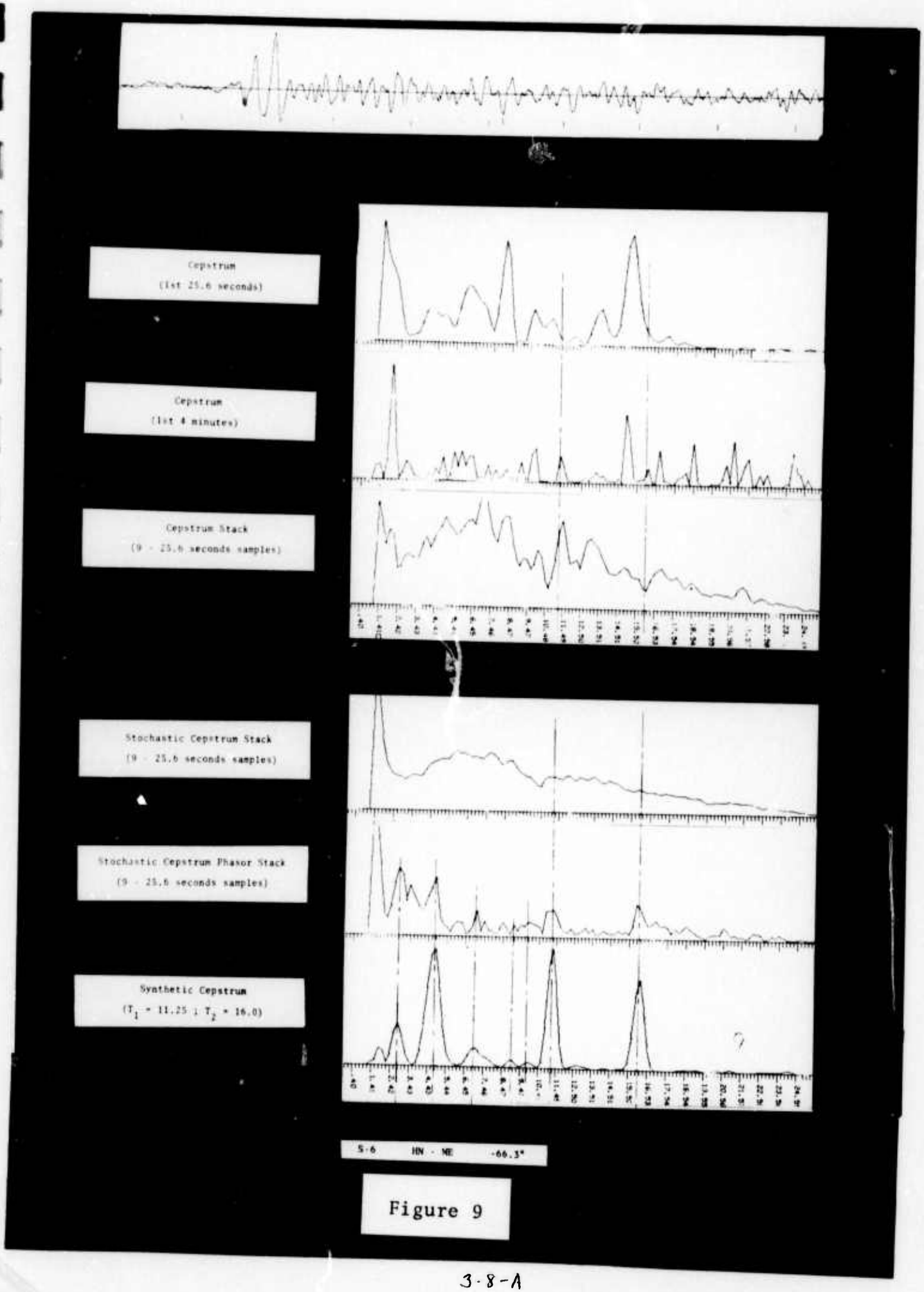
Cepstrum
(1st 25.6 seconds)
Cepstrum
(1st 4 minutes)
Cepstrum Stack
(9 - 25.6 seconds samples)
Stochastic Cepstrum Stack
(9 - 25.6 seconds samples)
Stochastic Cepstrum Phasor Stack
(9 - 25.6 seconds samples)
Synthetic Cepstrum
(T_1 = 11.25 ; T_2 = 16.0)
5-6 HN - ME -66.3°

Figure 9

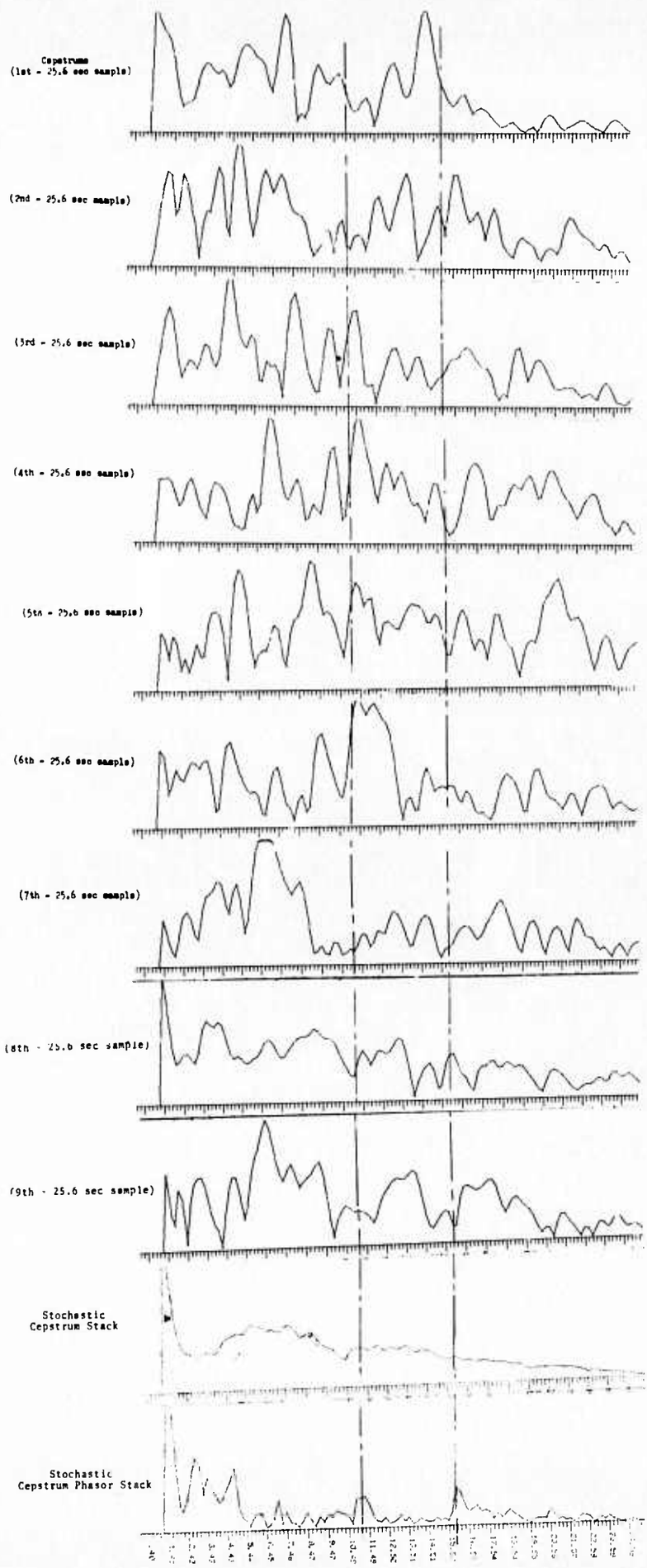

Cepstrum Stack Components of data from HN-ME

3-8-B

Figure 10

component cepstrums, one does not see evidence of a peak. This is dramatic evidence of how the phase information can aid in detection; for in this case it is the consistency of the phase of these phasors and not their amplitudes which give rise to a dominant peak in the phasor summation. This technique shows great promise and should be investigated further. Modifications such as increasing the phase selectivity can easily be worked into this technique.

In Figure 11 the results for EN-MO are plotted. For this station there is no indication of a depth phase at the expected delay time from either the visual or conventional methods shown in Figure 11. (In Figure A-6 are plotted 14 consecutive 25.6 second cepstrums for EN-MO.) Only the stochastic cepstrum stack and the stochastic cepstrum phasor stack give a dominant peak at the pP delay time.

In Figures 12-14 are results for stations HV-MA, KN-UT, and JP-AT, which lie in the Rocky Mountains. Depth phase detection was not successful at these stations using any of the methods.

A summary of the results for the individual station analysis are seen in Figures 15 and 16. In Figure 15 are the results for all six stations using methods 1 and 3. There is little evidence of dominant peaks appearing at the expected delay times. Figure 16 summarizes the results of the stochastic stacking and stochastic phasor stacking techniques. Here, although not overwhelming, is evidence developing for a depth phase detection.

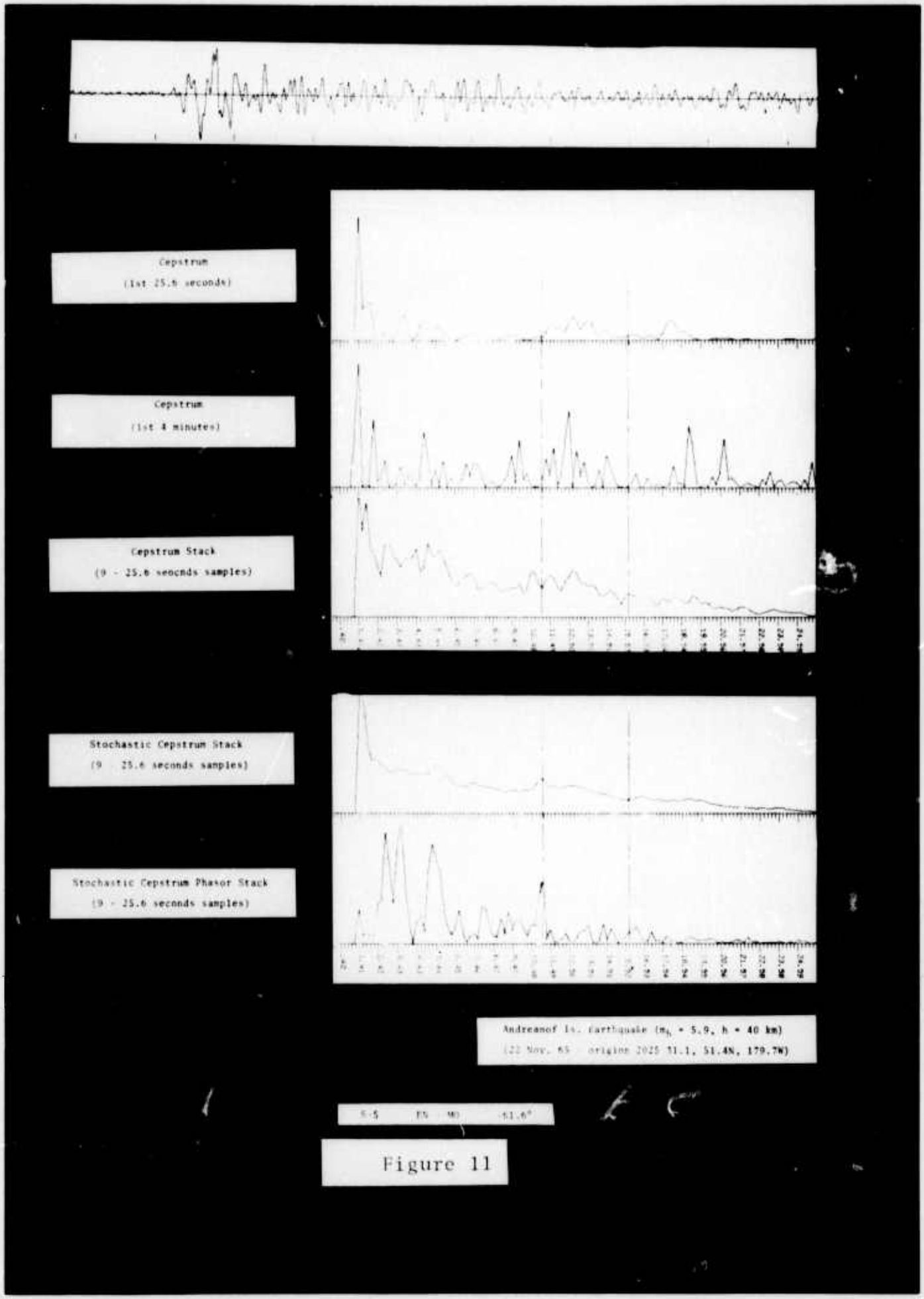
Cepstrum
(1st 25.6 seconds)
Cepstrum
(1st 4 minutes)
Cepstrum Stack
(9 - 25.6 seocnds samples)
Stochastic Cepstrum Stack
(9 - 25.6 seconds samples)
Stochastic Cepstrum Phasor Stack
(9 - 25.6 seconds samples)
Andreanof Is. Earthquake (m$_b$ = 5.9, h = 40 km)
(22 Nov. 65 origine 2025 51.1, 51.4N, 179.7W)

Figure 11

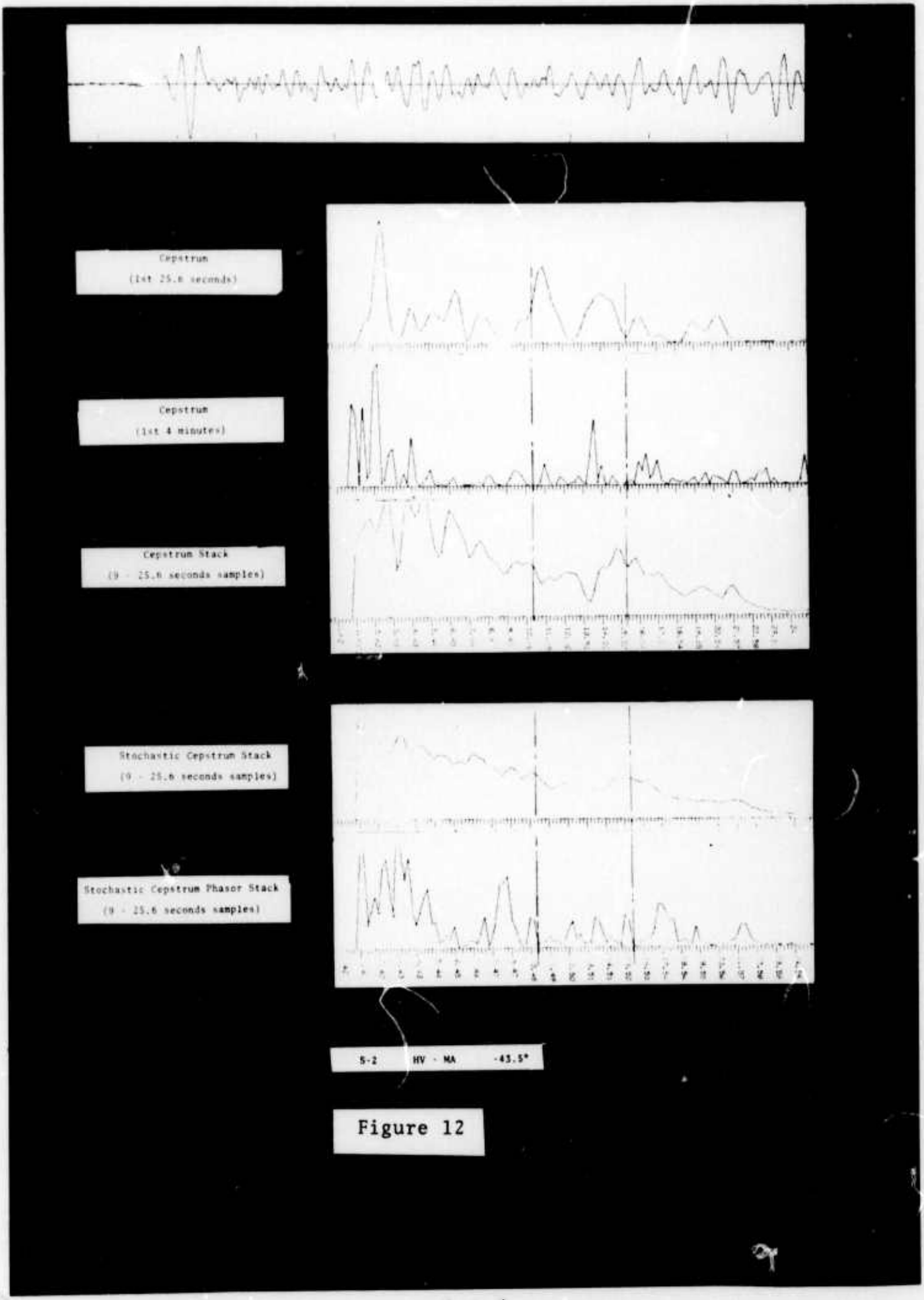
Cepstrum
(1st 25.6 seconds)
Cepstrum
(1st 4 minutes)
Cepstrum Stack
(9 - 25.6 seconds samples)
Stochastic Cepstrum Stack
(9 - 25.6 seconds samples)
Stochastic Cepstrum Phasor Stack
(9 - 25.6 seconds samples)
S-2 HV - MA -43.5°

Figure 12

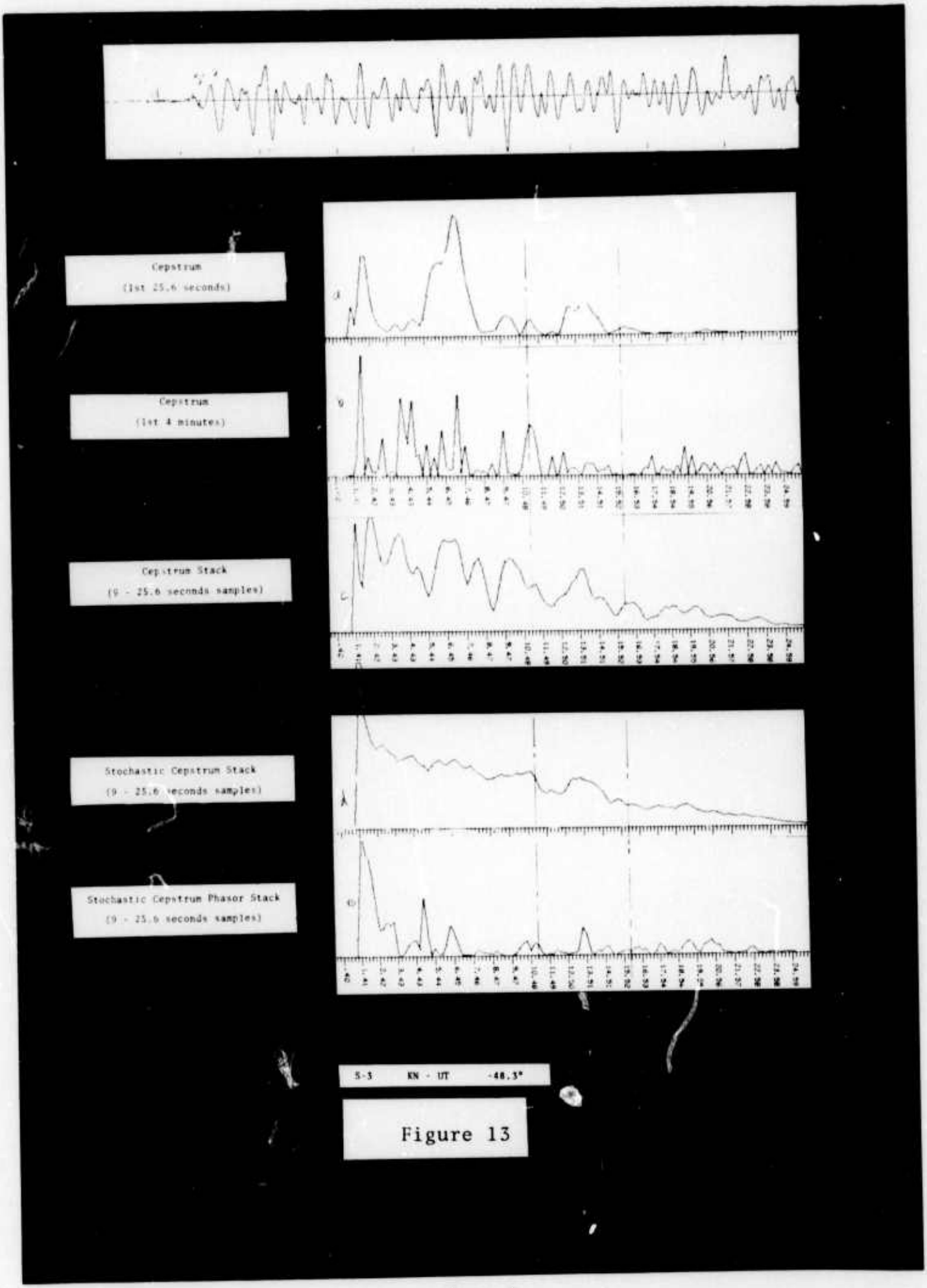
Cepstrum
(1st 25.6 seconds)
Cepstrum
(1st 4 minutes)
Cepstrum Stack
(9 - 25.6 seconds samples)
Stochastic Cepstrum Stack
(9 - 25.6 seconds samples)
Stochastic Cepstrum Phasor Stack
(9 - 25.6 seconds samples)
S-3 KN - UT -48.3°

Figure 13

Cepstrum
(1st 25.6 seconds)

Cepstrum
(1st 4 minutes)

Cepstrum Stack
(9 - 25.6 seconds samples)

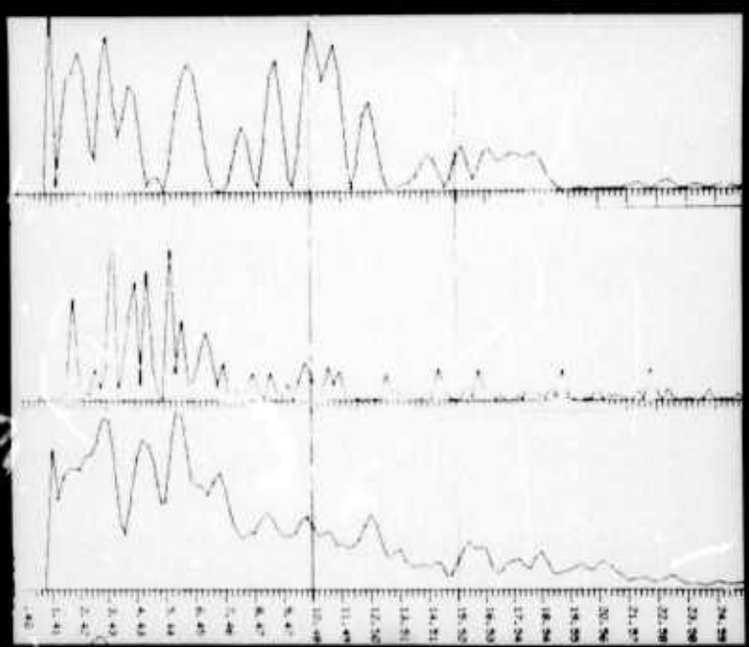

Stochastic Cepstrum Stack
(9 - 25.6 seconds samples)

Stochastic Cepstrum Phasor Stack
(9 - 25.6 seconds samples)

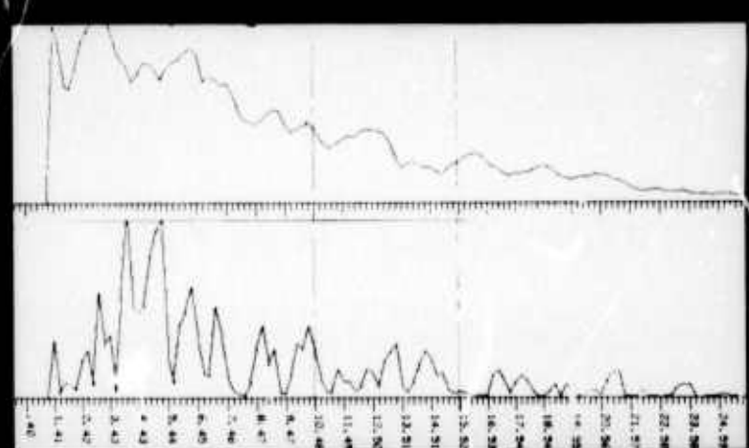

S-4 JP-AT 36.8°

Figure 14

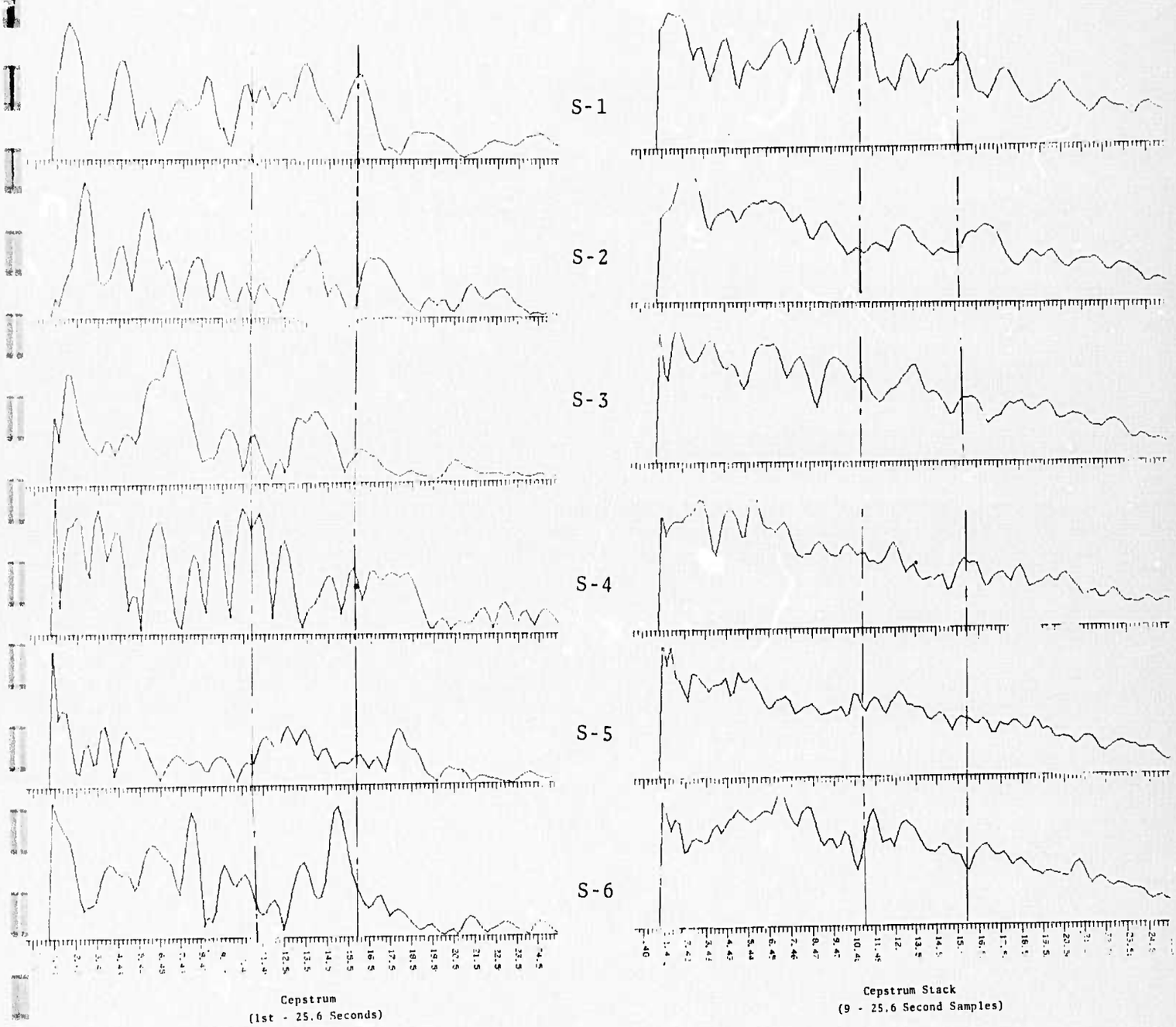

Summary of results of the 25.6 second cepstrum and the Cepstrum Stack

Figure 15

3-9-E

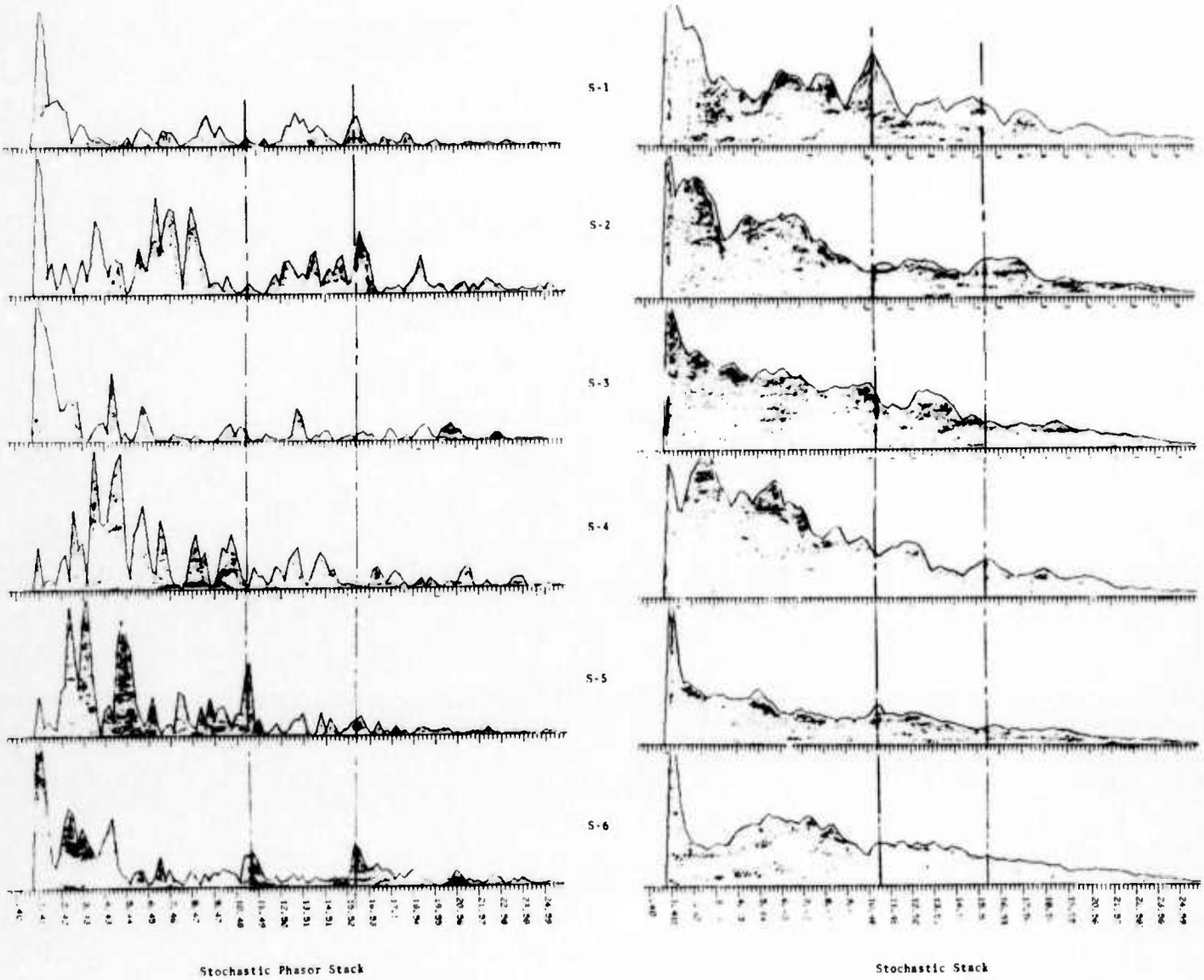

Summary of Results from the Stochastic Stack and the Stochastic Phasor Stack

Figure 16

In Figure A3 of the appendix are plotted the auto-correlations of the low pass filtered (cutoff frequency is equal to the inverse of the stochastic time window) seismograms for five of the stations. To calculate these auto-correlations the N sampled amplitude values ($X_M(n)$, (n=0,1, ..., N-1) were low pass filtered using a running average,

$$X'_M(j) = \frac{1}{2K+1} \sum_{k=-K}^{K} X_M(j-k)$$

where K is set at 10 such that the cut off frequency is approximately equal to the inverse of the stochastic time window. N zeroes were then added to X'_M to avoid wrap around problems and the correlation function $C_M(k)$ for positive lags was then calculated from

$$P_M(j) = \left| \frac{1}{2N} \sum_{n=0}^{2N-1} X'_M(n)\, e^{-2\pi ijn/2N} \right|^2, \quad j=0,1,\ldots,2N-1$$

$$CC_M(k) = \frac{1}{2N} \sum_{j=0}^{2N-1} P_M(j)\, e^{-2\pi ijk/2N}, \quad k=0,1,\ldots,N-1$$

$$C_M(k) = \sum_{M=1}^{NS} CC_M(k) \cdot W_M \; ; \quad k=0,1,\ldots,N-1$$

In Figure A4 of the appendix are plotted the cepstrum stack of the low pass filtered seismograms, where a pP detection similar to the one obtained by the stochastic techniques is apparent for MN-NV. This is the only case in which one of the conventional techniques gave rise to a dominant peak at an expected delay time. For this case low pass filtering had much the same effect as the stochastic windowing. Figure A5 of the appendix shows the combined best results of methods 4 and 5. Also tried but not plotted was analysis using low pass filtered data with the phasor technique without using stochastic stacking. This method was not successful for any of the six stations.

Summarizing the results of all methods discussed so far, depth phase detection was achieved at three of the six stations (one of which gave both pP and sP) using the new techniques, whereas the conventional methods achieved pP detection at one station.

3.2 Depth Phase Detection Using Combined Data from Several Stations

Next we show how further improvements in depth phase detection can be achieved by using the combined data of several stations.

Return to Figure 16 where one observes that for stations HV-MA, MN-NV, KN-NT, pP is detected at only MN-NV and sP is not detected at any of these stations using stochastic stacking. For each of these stations we calculated

an equal number of cepstrums from consecutive 25.6 second portions of the seismograms. In Figure 17 are the results of stochastically averaging these cepstrums of these stations using different coda lengths (the trend has been removed from the averaged cepstrum plotted). These three stations are at approximately the same distance from the event (~45°). We note a clear detection of both the pP and sP delay times when 5.0 minutes of the codas is used. Also, note that the detection of pP and sP improves as more of the information contained in the coda is used. This is evidence that these stochastic techniques are making constructive use of the additional seismic depth phase information contained in the coda. (Similar results were obtained by stochastically stacking the cepstrum phasors of the three stations.)

The results can be further improved with the addition of the seismic data recorded at the stations EN-MO, and HN-ME. In Figure 19 are the results of averaging data from the five stations HV-MA, MN-NV, KN-UT, EN-MO and HN-ME using coda lengths ~2.5 and ~5.0 min. We obtain a clear detection of pP using 2.5 min. of the coda and by using 5.0 min. the sP detection becomes clear. But note that the two additional stations are at 62° and 66° compared with ~45° for the other three. The cepstral peak position would therefore be expected to differ by ~.5 seconds between the two sets of stations. One can adjust for these station distance differences by shifting the cepstrums for EN-MO and HN-ME by ~-.5 seconds before stacking. A further improvement in clearity in the detection of pP and sP delay times is then observed from Figure 19.

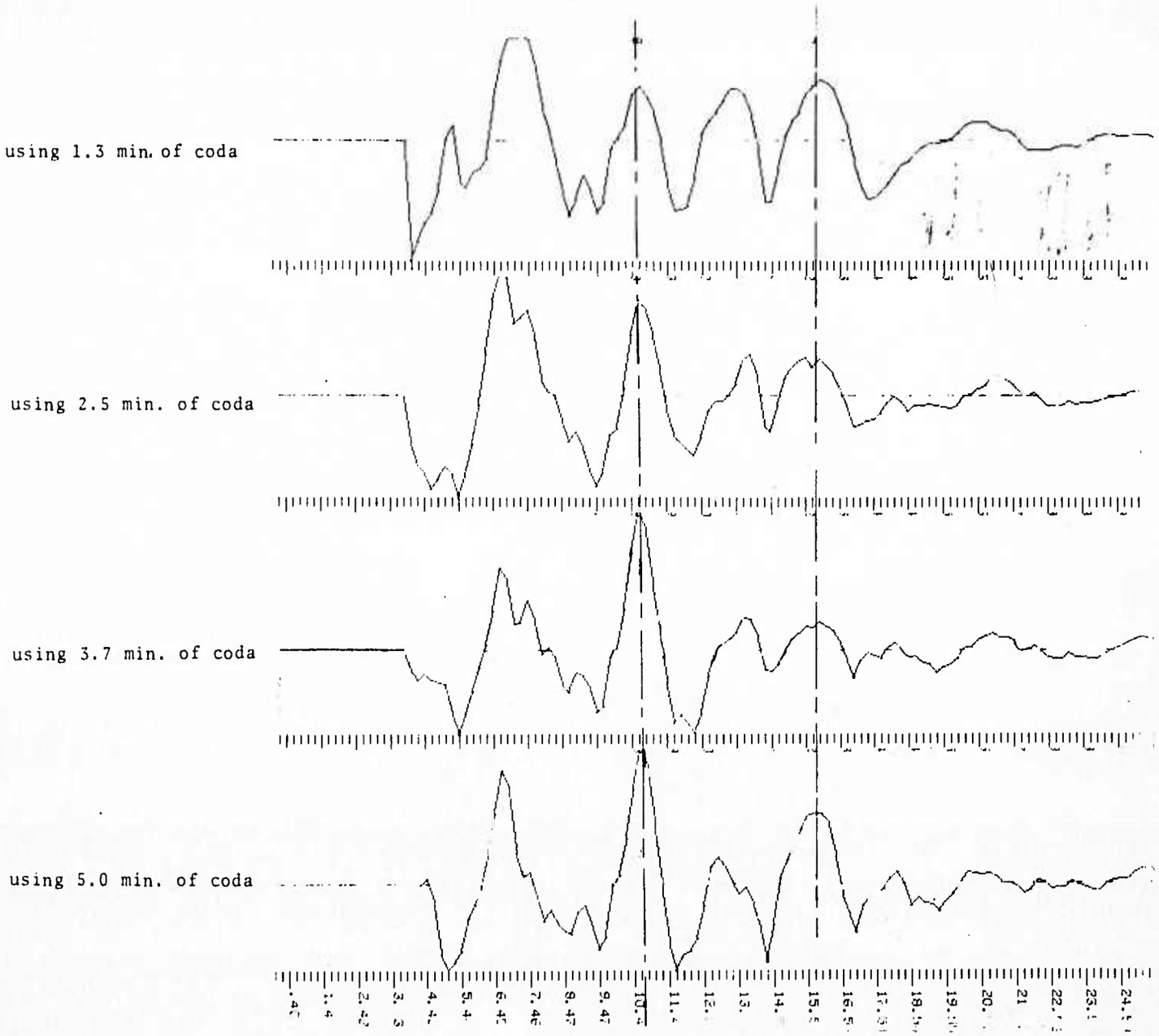

Stochastic cepstrum stack using 25.6 seconds samples of the 3 stations HV-MA, MN-NV, KN-UT

Figure 17

3-12-A

The results shown in Figure 18 are very encouraging since we have obtained an excellent detection of the pP and a good detection of the sP delay times for an event in which both the visual and the standard techniques, which we investigated, gave very little indication of the presence of these phases. These results also give promise of significant improvements in depth phase detection for small events having poor signal to noise ratios when these events are recorded at several stations. The stochastic averaging allows one to make constructive use of information contained in the codas recorded at different stations as well as different portions of a given coda.

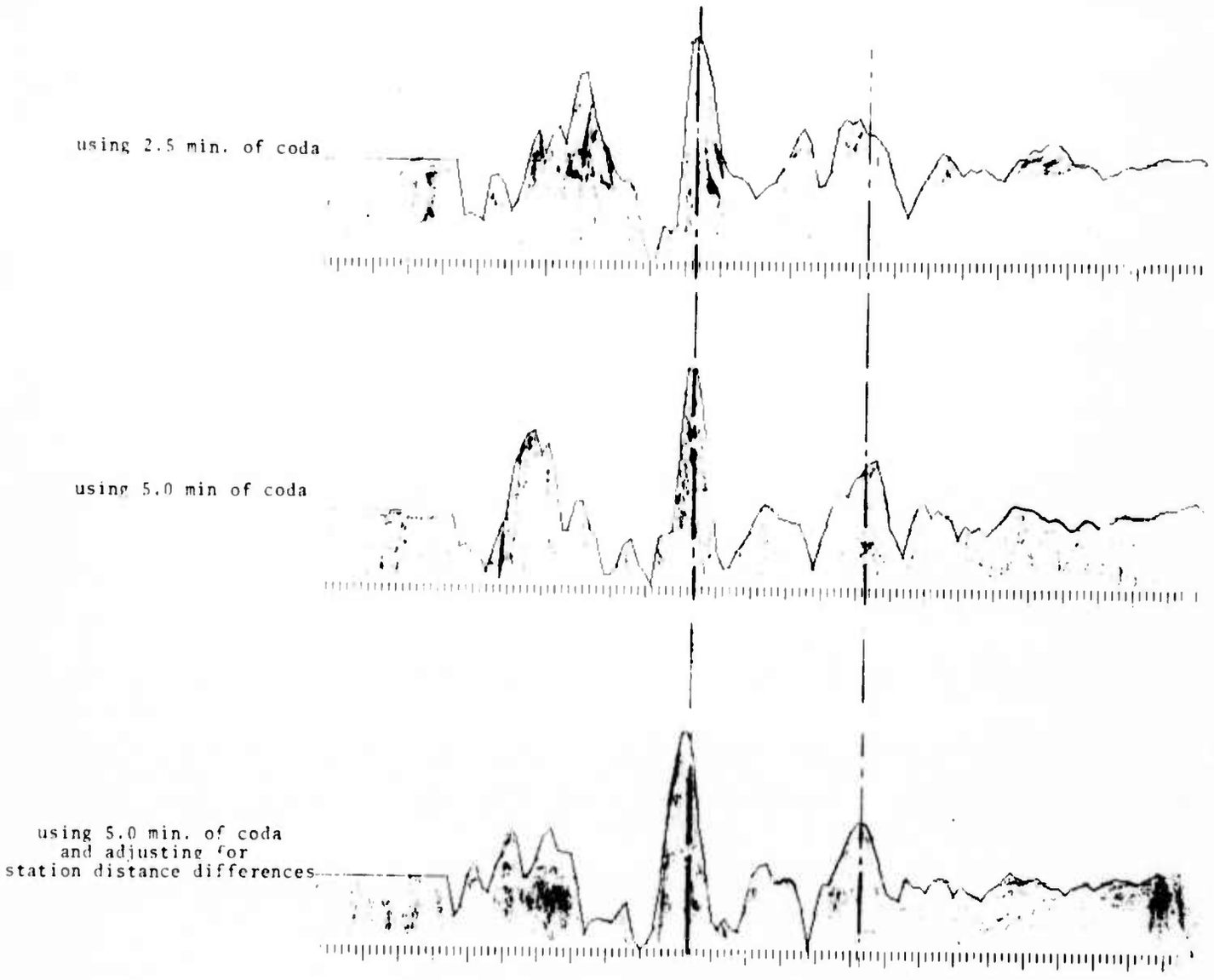

Stochastic cepstrum stack using 25.6 seconds samples
of the 5 stations HV-MA, MN-UV, KN-UT, EN-MO, HN-ME

Figure 18

4.0 CONCLUSION

This research effort has been directed at determining whether certain new statistical signal processing techniques, applied to the entire seismogram, could significantly enhance seismic depth phase detection. The new analysis techniques allow one to make constructive use of the additional depth phase information contained in the coda, rather than restricting the analysis to the first arrival portion of the seismogram. Results of the analysis of a single event at six stations indicates that major improvements in depth phase detection are possible.

Two new techniques were introduced in the depth phase analysis. The first of these techniques allows for depth phase delay time variations associated with the later seismic arrivals comprising the coda. The second of these techniques utilizes the phase consistency between the direct and surface reflected seismic arrivals.

For the event analyzed the depth phases were not visually identifiable from the seismogram. Results of the cepstral analysis incorporating these two new techniques gave rise to dominant cepstral peaks, for three of the six stations, which were consistent with a 39 km deep event. At one of the stations the entire cepstral pattern expected for a seismogram containing the pP and sP arrivals was obtained. These results were compared

with the analyses using several conventional depth phase detection techniques including the cepstrum, stacked cepstrums, auto-correlations and low pass filtering the seismograms before performing these analyses. One of the conventional techniques gave rise to an indication of the pP delay time at one of the stations similar to that obtained by the new techniques.

Results of stochastically averaging the data from several stations demonstrated detection of depth phases which were not apparent from analysis at any of the individual stations. These results also clearly indicated how the depth phase detection improved as more of the coda was used in the analysis.

The new depth phase detection techniques have been thus far applied to only a single event. The analysis gave clear indications of pP and sP delay times consistent with a 39 km deep event and represented a major improvement over conventional techniques for this case, however, the depth of this event was not considered to have been conclusively established. The next research effort should therefore be to apply these new techniques to a suite of events having well established depths and to further develop these techniques using this data.

APPENDIX

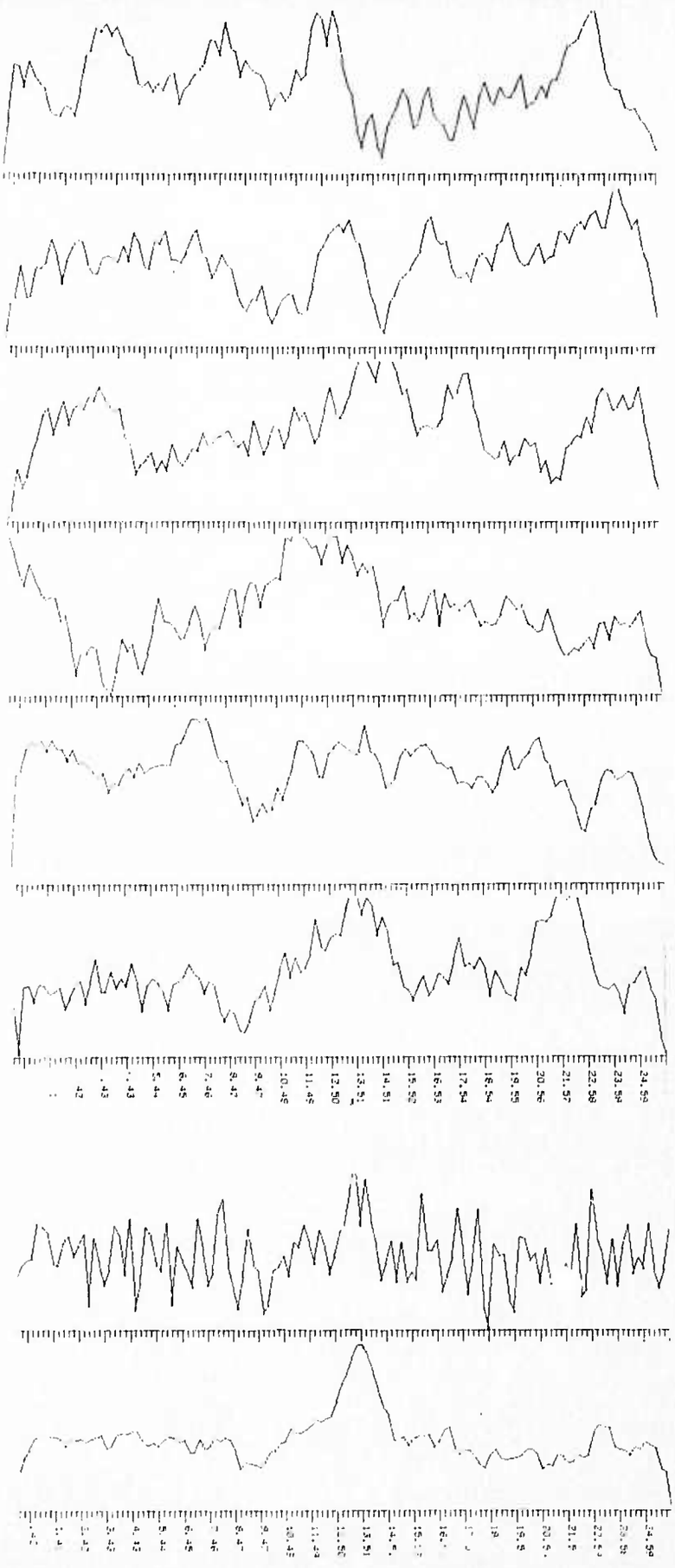

Demonstration nf stochastic stacking
using low pas filtered synthetic data

Figure A-1

5-9

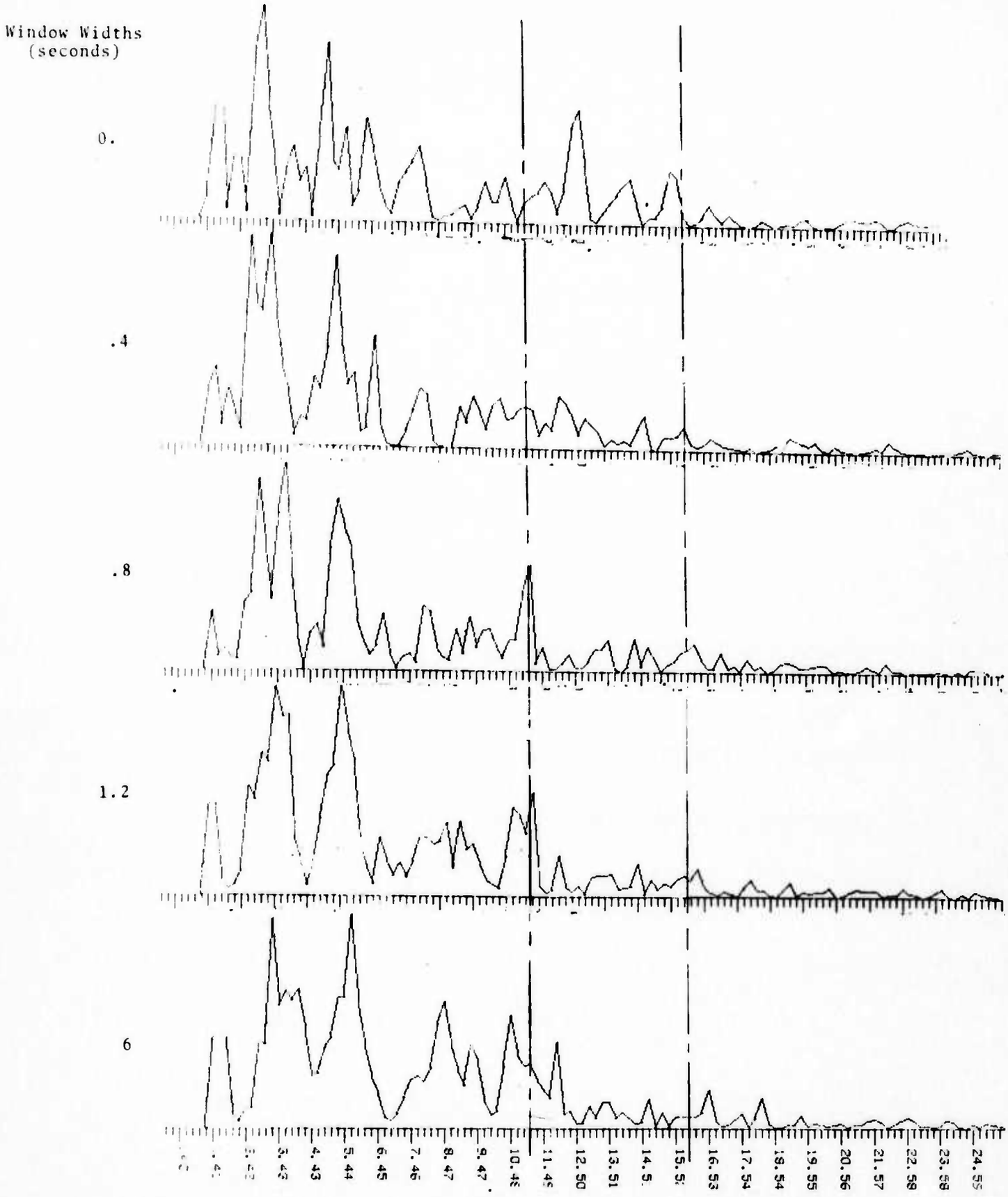

Stochastic cepstrum phasor stack for various stochastic window widths (EN-MO)

Figure A-2

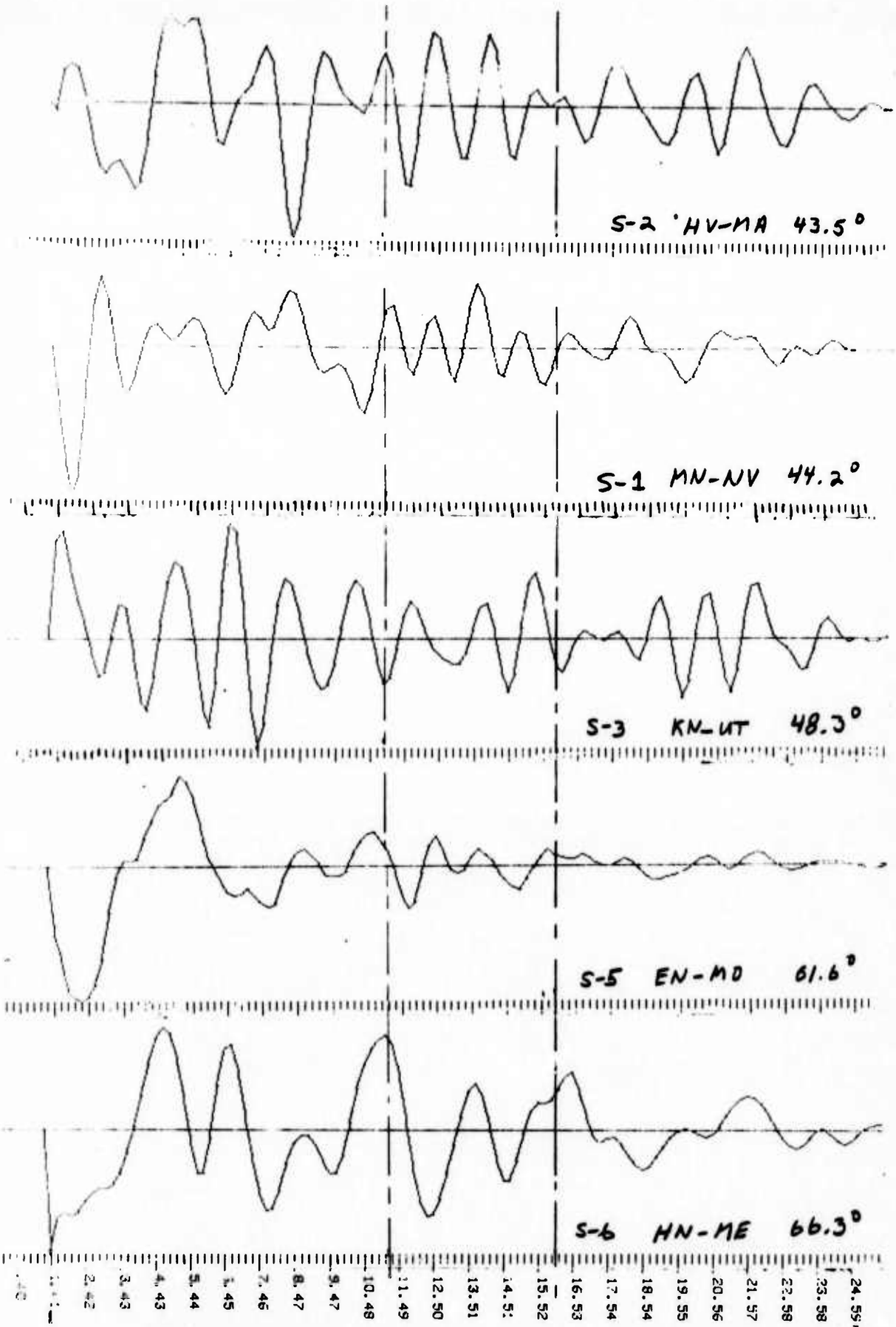

Auto-Correlation Stack of Low Pass Filtered Data
(9-25.6 second samples)

5-4

Figure A-3

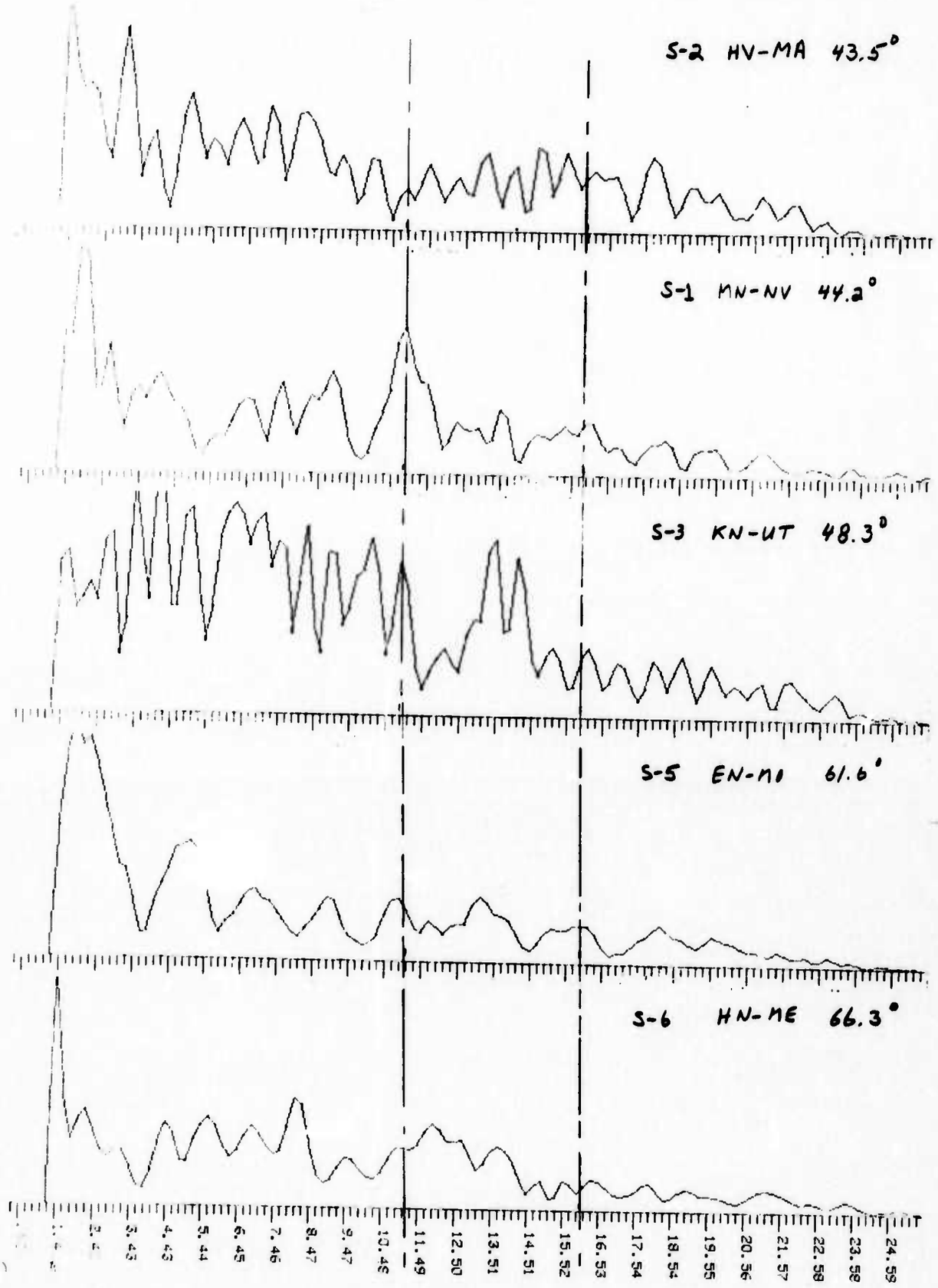

Cepstrum Stack of Low Pass Filtered Data
(9 - 25.6 second samples)

Figure A-4

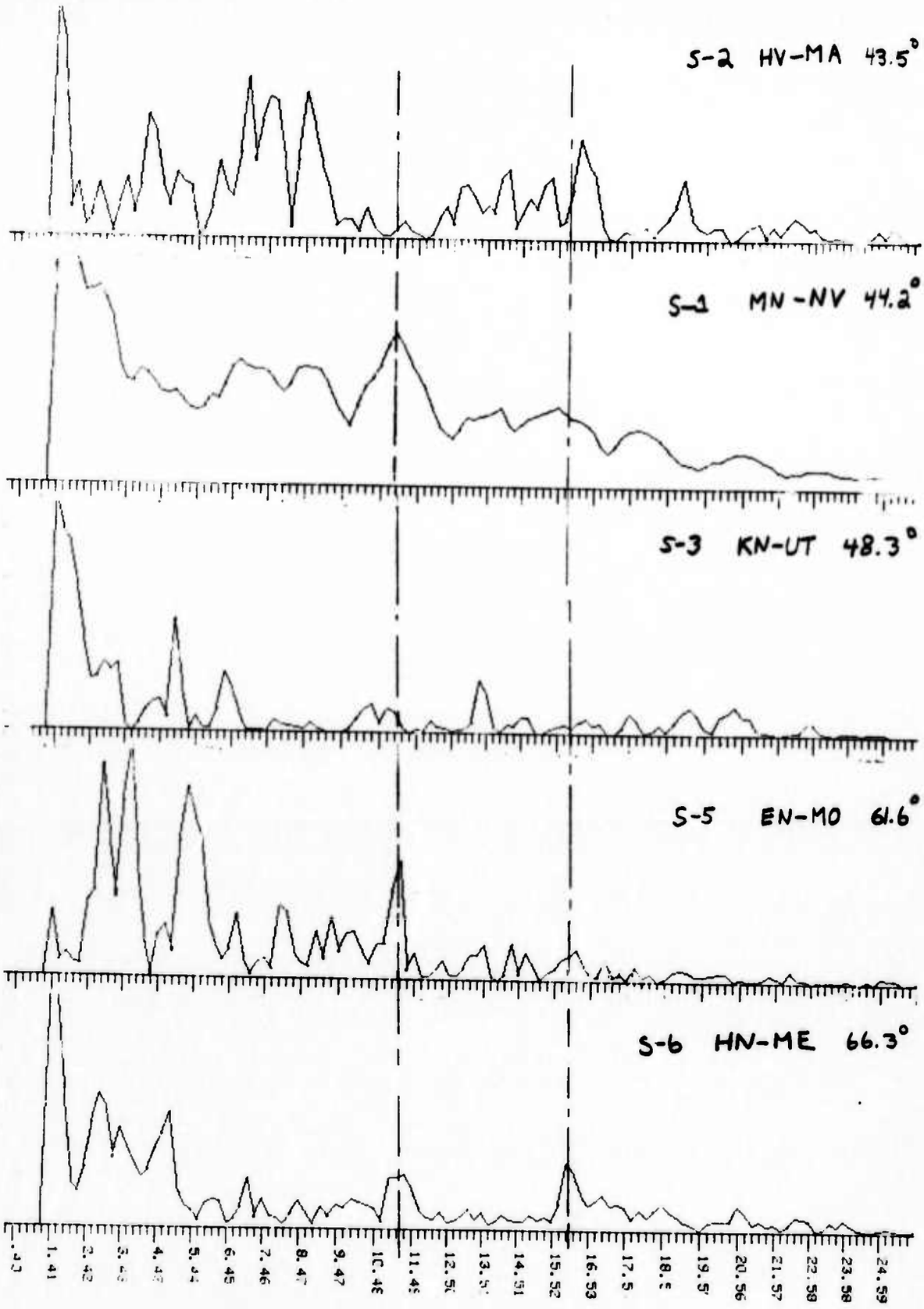

Combined best results of the stochastic cepstrum stack and stochastic cepstrum phasor stack techniques (9 - 23.6 second samples)

Figure A-5 5-5

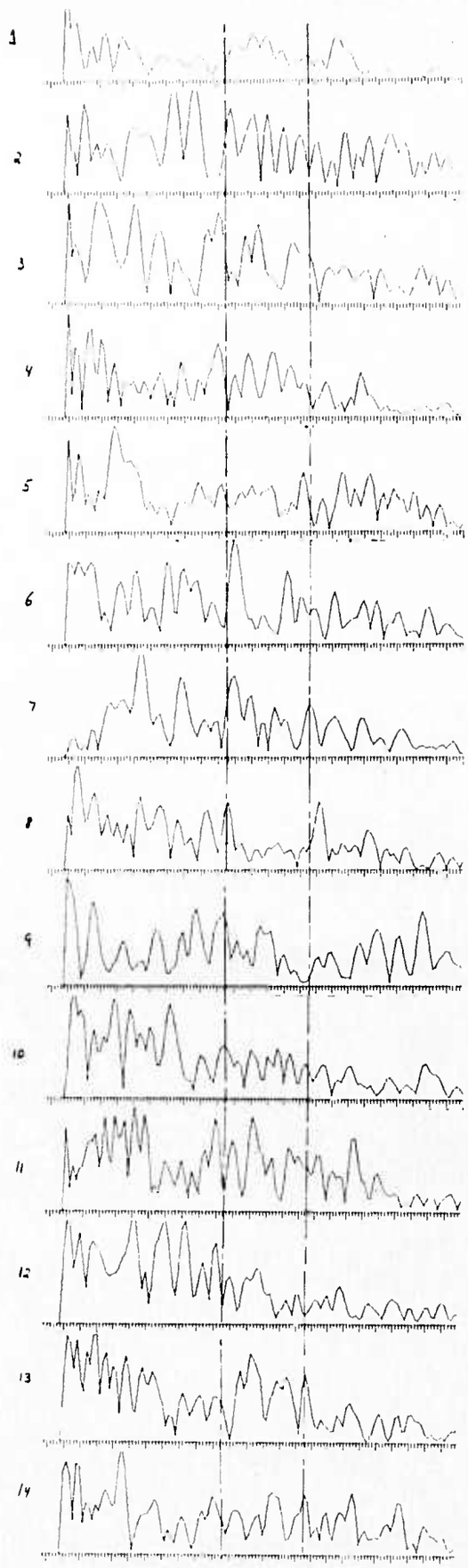
1
2
3
4
5
6
7
8
9
10
11
12
13
14
Consecutive Cepstrum (25.6 Seconds Each) EN-MO

Figure A-6

REFERENCES

1. B.P. Bogert and J.F. Ossanna, "The Heuristics of Cepstrum Analysis of a Stationary Complex Echoed Gaussian Signal in Stationary Gaussian Noise", Transactions on Information Theory, Vol. IT-13 No. 3, pp. 373-380, July 1966.

2. B.P. Bogert, M.J.R. Healy, John W. Tukey, "The Quefrency Analysis of Time Series for Echoes: Cepstrum, Pseudo-Autocovariance, Cross-Cepstrum and Saphe Cracking", Rosenblatt, M., ed. "Time Series Analysis", New York, Wiley, 1963.

3. R.E. Ingram, S.J., and J.H. Hodgson, "Phase Change of PP and pP on Reflection at a Free Surface", BSSA, pp. 203-212, Nov. 1955.

4. H.S. Hasegawa, "Short Period P-Coda Characteristics in the Eastern Canadian Shield", BSSA, Vol.60, No.3, pp. 839-858, June 1970.